

Chapter 10

DEPENDENCE OF RETINAL THERMAL INJURY THRESHOLD ON SIZE AND PROFILE OF LASER IMAGE

DAVID J. LUND, BA*; RICHARD C. HOLLINS, DPHIL[†]; AND KARL SCHULMEISTER, PHD[‡]

INTRODUCTION

BACKGROUND

- Issues of Laser Safety
- Image Size
- Influence of Refractive Errors on Image Size
- Image Diameter

LASER SAFETY GUIDELINES

HISTORICAL EMPIRICAL BASIS FOR LASER SAFETY GUIDELINES

PHYSICAL MODELS AND CALCULATIONS

- Simple Models
- Computer Models
- Model Results
- Variations to Fit the Small Spots
- Images With Complex Profiles

DISCUSSION AND CONCLUSIONS

SUMMARY

*Research Biophysicist (Retired), US Army Medical Research Detachment, 7965 Dave Erwin Drive, Brooks City-Base, Texas 78235

[†]Senior Fellow, Cyber and Information Systems Division, Defence Science and Technology Laboratory, Porton Down, Salisbury, SP4 0JQ, United Kingdom

[‡]Consultant on Laser and Optical Radiation Safety, Seibersdorf Laboratories, Seibersdorf, Austria

INTRODUCTION

The relationship between the threshold for thermally induced injury of the retina and the size and shape of the retinal image (area of laser exposure) has been a topic of discussion for many years. For lasers in the retinal hazard wavebands, this question is central to the understanding and application of laser safety exposure limits. However, the relevant experiments and their interpretations are problematic, and the evolution of experimental techniques has generated an assortment of datasets that are difficult to reconcile. Safety standards have contained anomalies that are not explicable by physical models, and their accuracy has been questioned in light of data that have become available over the past 15 years. This chapter reviews experimental techniques used in these studies, study data, relevant physical models, and previous and current safety standards. After much debate, our understanding has converged toward a revision of the dependence of the exposure limits on image size.

Several issues complicate the interpretation of in-vivo threshold data involving different image sizes. Image size at the retina is not directly measurable, so it must be inferred from the measured characteristics of the incident beam (the laser beam to which the eye has been exposed) and assumptions about the optical quality and transparency of the eye and its state of accommodation (whether it is focused on a near or far object). Errors may be introduced at this stage, particularly for small images. Moreover, lesion observation is influenced by lesion size, which may differ from the size of the laser image itself. As the image size is adjusted, the observed dependence of the injury threshold can be influenced by all of these issues. Thus, it becomes difficult to accurately identify trends in the injury threshold. In-vitro experiments¹⁻⁴ enable better control over the size of the image and

the detection of lesions, but questions remain about whether these data correctly reflect the dependencies of in-vivo laser-tissue interactions.⁵

The understanding of the laser-tissue interaction has itself been revised, particularly for short laser pulses (see Chapter 12, Ultrashort Lasers and Their Bioeffects, this volume). As pulse duration is reduced to below $\sim 10 \mu\text{s}$, bubble generation and other mechanical processes begin to accompany the thermally induced reactions that cause injuries from longer pulses.^{6,7} Serious attempts to model the injury threshold's dependence on image size have been confined to thermal processes,⁴ and even then, some difficulty remains in reconciling the models with all of the parametric dependences, especially for small image sizes.

In the past, safety standards have been based largely on in-vivo experiments done before 1980. These early studies, conducted in a number of laboratories, covered a wide variety of wavelengths and pulse durations. However, image diameters addressed in each study were usually confined to just two or three widely separated data points. Findings revealed some anomalies, so substantial safety margins were built into the safety standards to compensate. More recent experiments have investigated significant wavelengths and pulse durations in greater detail, with closer-spaced image sizes. These more stringent experiments indicate deficiencies in the previous safety standards. Under certain exposure conditions, safety margins have been eroded or even eliminated by differences between the parametric dependences apparent in the new data and those built into the earlier standards. This chapter will consider these issues with attention to laser safety, emphasizing the use of advanced models and improved experimental techniques to resolve dataset differences.

BACKGROUND

Issues of Laser Safety

Retinal image size is heavily influenced by exposure conditions, and for a given intraocular power, retinal irradiance varies according to the inverse square of the image diameter. Direct ocular exposure to a well-collimated, coherent beam usually produces a small, tightly focused retinal image. However, when, for example, a beam is scattered by a diffusing screen, it produces a much larger retinal image whose size is determined by geometrical optics rather than by the coherence of the beam. The area of the resulting image can vary by a factor greater than 1,000. Between

these two extremes, a range of image sizes is possible, controlled by the divergence and coherence of the incident beam and by the state of accommodation of the eye. The resulting wide variety of image sizes can be produced in controlled experiments or by accidental exposures on the battlefield or elsewhere.

The study of the relationship between retinal image size and light-induced retinal injury thresholds is important to safety for several reasons. First, scaling laws are built into safety standards. Experimental and theoretical studies are essential to test our understanding of underlying processes. Second, a better understanding can provide a "bridge" between safety standards for

lasers and incoherent light sources. The two sets of standards should merge seamlessly as the size of the retinal image varies. Finally, there is potential protective benefit. Ocular hazard can be reduced considerably by degrading the focusability of the beam.

Image Size

Image size, or more precisely the diameter of the irradiated area on the retina and the distribution of irradiance or radiant exposure across that diameter, is by far the least accurately quantified and understood variable affecting the threshold for laser-induced retinal damage. Parameters of the laser beam incident at the cornea can be precisely controlled and measured, and the laws of geometric optics and physical optics can be applied to the transmission of the beam through the ocular optics. However, because the eye is a biological system, it is capable of perturbing the transmitted beam and the distribution of irradiance at the retina in unexpected and unrecognized ways.

For direct intrabeam exposures of anesthetized animals accommodated to infinity (focused on a far object), the diameter, D , of the retinal image is controlled principally by the divergence, α , of the intraocular beam. The relationship between D and α is illustrated most easily for the so-called "Maxwellian view" exposure geometry, in which the beam is brought to a focus at the pole of the ocular system, as shown in Figure 10-1.

In this case, all rays are effectively undeviated, and the size of the image on the retina is

$$(1) \quad D = f\alpha$$

where f is the effective focal length of the eye. In practice, this simple geometry is never used in exposure experiments due to the risk of unwanted injury at the focus of the beam. Instead, experiments use a "modified Maxwellian view" geometry, in which the focus is usually positioned a distance, Z , in front of the eye, as shown in Figure 10-2, where Z is often adjusted so that the incident beam at the pupil has a diameter of 3 to 4 mm.

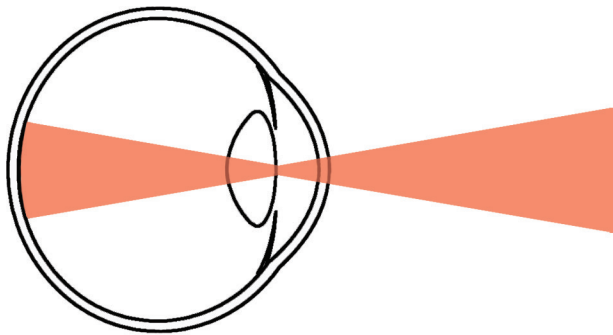


Figure 10-1. The "Maxwellian view" exposure geometry for irradiation of large retinal areas.

If the refractive state of the eye is adjusted to focus distant objects, the retina will be one focal length away from the pole, and the simple construction shown in Figure 10-2 shows that despite displacement Z , the size of the retinal image is still given by equation (1). In general, the image in the focal plane of a lens is directly related to the far-field irradiance distribution of the beam passing through the lens. Because the angle subtended by the far-field irradiance profile is the divergence, the angular subtense, α , of the image in the focal plane of the lens is also equal to the divergence.

If the refractive state of the eye is adjusted to focus distant objects, the retina will be one focal length away from the pole, and the simple construction shown in Figure 10-2 shows that despite displacement Z , the size of the retinal image is still given by equation (1). In general, the image in the focal plane of a lens is directly related to the far-field irradiance distribution of the beam passing through the lens. Because the angle subtended by the far-field irradiance profile is the divergence, the angular subtense, α , of the image in the focal plane of the lens is also equal to the divergence.

Influence of Refractive Errors on Image Size

Refractive errors have their maximum influence in the "smallest image" case. If the state of accommodation is not adjusted for optimum focus of the collimated beam, the resulting retinal image will be enlarged. According to simple geometrical optics, an otherwise perfect eye that exhibits an error in optical power, ΔP , in its anesthetized state will, for a collimated input beam, produce a retinal image of diameter

$$(2) \quad D_{min} \sim d_{beam} f_0 \Delta P$$

where d_{beam} is the diameter of the incident beam, and f_0 is the optical length of the eye (which is not equal to its focal length because of the refractive error). For

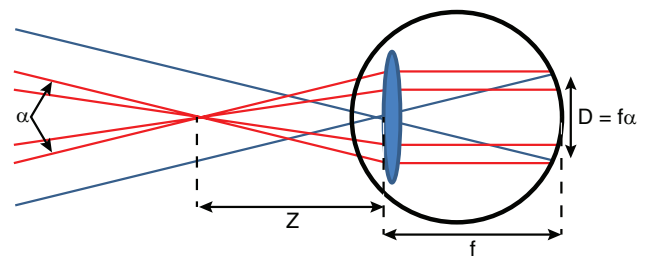


Figure 10-2. Modified "Maxwellian view" geometry for irradiation of large retinal areas with limited radiant exposure at the cornea. D : diameter; f : effective focal length of the eye; Z : focus distance in front of eye; α : angular subtense of the source.

Content includes material subject to © Crown copyright (2004), Dstl. This material is licensed under the terms of the Open Government Licence except where otherwise stated. To view this license, visit <http://www.nationalarchives.gov.uk/doc/open-government-licence/version/3> or write to the Information Policy Team, The National Archives, Kew, London TW9 4DU, or email: psi@nationalarchives.gsi.gov.uk.

a typical rhesus monkey exposure in which $d_{\text{beam}} = 3$ to 4 mm, $f_0 = 13.5$ mm, and $\Delta P = 0.25$ diopter, D_{min} is predicted by equation (2) to be about 10 to 13 μm .

For modified Maxwellian view exposures, the refractive error is usually less important. It modifies the image size to

$$(3) \quad D \sim f_0 a(1 + Z\Delta P)$$

The fact that ΔP appears in a minor linear term in equation (3) means that positive and negative refractive errors can compensate for each other in the statistical distribution among different subjects. This contrasts with the “smallest image” case, where refractive errors of either sign can only *increase* the image size. The $Z\Delta P$ term becomes most important for small images, because these involve the maximum values of Z . For example, for exposures with $\alpha = 5$ mrad, Z might be ~ 0.5 m in order to make $d_{\text{beam}} \sim 3$ mm at the pupil. If ΔP lies within ± 0.25 diopter, then $Z\Delta P$ will be in the range ± 0.13 for individual subjects, and averaging over subjects will probably reduce the effect on the average image diameter to less than $\pm 10\%$. The corresponding retinal irradiance would not be affected by more than $\pm 20\%$. Refractive errors rapidly become much less important for larger images.

Refractive errors vary from subject to subject, and most animal studies minimize their impact through preexposure ophthalmic screening. Skilled ophthalmologists can determine the refractive error to a precision of ± 0.25 diopter, and they normally accept errors estimated within the range ± 0.25 diopter. Most of the eyes accepted for study therefore have errors no greater than ± 0.25 diopter, although a small proportion may have errors of up to ± 0.5 diopter. Care is taken in the selection of subjects to ensure that each statistical threshold determination includes eyes with positive and negative refractive errors. It should be noted that refractive errors determined by ophthalmic screening do not necessarily map exactly into exposure experiments because laser energy absorption may occur deeper in the retina. Nevertheless, a refractive error of 0.25 diopter would move the focus axially by 45 μm , considerably greater than the thickness of the retinal pigment epithelium (RPE).^{8,9}

Image Diameter

The smallest retinal images are produced using a collimated beam. Equation (1) can no longer be used to determine the image size, which in these cases is limited by other issues. In the real eye, optical aberrations increase the retinal image over the diffraction limit.⁹⁻¹¹ In spite of considerable study, the minimum image size is still a topic of debate.

Several approaches have been used to measure the image size produced at the retina by a collimated incident laser beam. Invasive techniques allow a direct measure of the spot size by effectively placing a detector at the plane of the retina. These techniques have produced results ranging from 7 to 13 μm in the rabbit¹² and from 8 to 40 μm in the rhesus monkey.^{13,14}

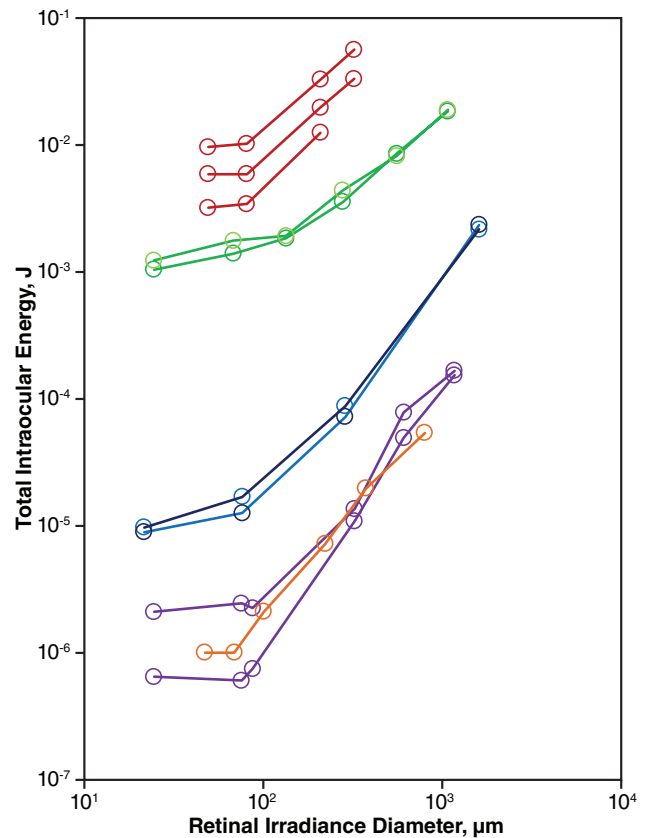


Figure 10-3. The dependence of ED_{50} on D for a range of exposure durations and laser wavelengths. *Orange:* 150 fs at 1,060 nm; *violet:* 5 ns at 532 nm; *blue:* 3 μs at 590 nm; *green:* 100 ms at 514 nm; *red:* 0.125 s, 0.5 s, and 1 s at 633 nm. Data sources: (1) Cain CP, Toth CA, Noojin GD, et al. Visible lesion threshold dependence on retinal spot size for femto-second laser pulses in the primate eye. *J Laser Applications*. 2001;13(3):125–131. (2) Zuclich JA, Edsall PR, Lund DJ, et al. New data on the variation of laser-induced retinal damage threshold with retinal image size. *J Laser Applications*. 2008;20(2):83–88. (3) Zuclich JA, Edsall PR, Lund DJ, et al. Variation of laser-induced retinal damage threshold with retinal image size. *J Laser Applications*. 2000;12(2):74–80. (4) Lund DJ, Edsall PR, Stuck BE, Schulmeister K. Variation of laser-induced retinal injury with retinal irradiated area: 0.1 s, 514 nm exposures. *J Biomed Opt*. 2007;12(2):06180. (5) Ham WT Jr, Geeraets WT, Mueller HA, Williams RC, Clarke AM, Cleary SF. Retinal burn thresholds for the helium-neon laser in the rhesus monkey. *Arch Ophthalmol*. 1970;84:797–809.

Photographic techniques simultaneously image the laser on the retina and an object of known size (such as a wire or bead inserted into the eye) or, alternatively, retinal blood vessels, which are measured after enucleation of the eye. In three animal studies, the laser image on the retina so measured has been reported to be $40\ \mu\text{m}$ ^{15,16} and $50 \pm 25\ \mu\text{m}$.¹⁷ Other researchers have reported an image size based on the size of the retinal lesion resulting from exposure. However, this approach is problematic because the lesion changes with time due to metabolic response to the injury; the resulting lesion may be larger than the laser image.

Historically, the distribution of light in human retinal images has been estimated by measurement of the line spread function, modulation transfer function, or point spread function.¹⁸⁻²¹ These measurements show that at least a portion of the retinal image can be as small as $6\ \mu\text{m}$, corresponding to an angular resolution of $0.35\ \text{mrad}$. However, this high-resolution component is surrounded by a broader scattered component. The available data suggest that the smallest retinal images are $\sim 20\ \mu\text{m}$.^{22,23} Most recently, techniques have evolved to measure the wave-front aberration errors of human eyes. Retinal image diameters have been estimated using ray-tracing software in a model eye

incorporating these wavefront errors. Retinal image diameters as low as $6\ \mu\text{m}$ are estimated for eyes with the least refractive error.^{11,24}

The above discussion shows that estimates of the image diameter in in-vivo experiments are likely subject to uncertainties that should be assessed carefully in light of what is known about the incident beam and exposure conditions. Many authors assign a nominal image diameter of $\sim 25\ \mu\text{m}$ to collimated-beam laser exposures in monkey subjects. Recent data suggest that the minimum diameter could be as large as 80 to $100\ \mu\text{m}$, based on the observation that the incident energy at the cornea required to produce retinal damage does not continue to decrease with D below that diameter (Figure 10-3).²⁵⁻²⁷ Sliney et al cite several factors that may cause the minimum achieved spot size to be greater than the expected values.⁹ These factors include small-angle forward scatter of the laser beam within the eye, which distributes the energy over a larger diameter than expected at the retina; larger than predicted uncompensated aberrations of the eye of the anesthetized monkey; and limited capability of the investigator to detect retinal alteration contained within diameters less than $100\ \mu\text{m}$ unless additional energy is introduced to produce a more severe and therefore more visible alteration. The combined effect of these factors might be significant.

LASER SAFETY GUIDELINES

Before 1986, the maximum permissible exposure (MPE) for viewing an extended laser source was expressed in units of source radiance or source-integrated irradiance, and was constant for any given combination of wavelength and exposure duration.²⁸ Retinal irradiance is proportional to the source radiance.^{23,29} Thus, the retinal irradiance at the MPE was a constant that required the total energy incident on the retina to vary directly with the area of retinal image; that is, the MPE, expressed as energy incident on the cornea within the area of the ocular pupil (total intraocular energy [TIE]), varied according to the formula $\text{MPE}_{(\text{TIE})} = kD^2$, where k is a constant relating the MPE at $D = D_0$ to the value D_0 . This simple provision was confounded by the idea that α_{min} , the limiting angular subtense that divides intrabeam (point-source) viewing from extended source viewing, was a function of exposure duration, reaching a minimum of $1.5\ \text{mrad}$ at $18\ \mu\text{s}$, and increasing for both shorter and longer duration pulses. The rationale for such behavior by α_{min} was unclear for durations shorter than $18\ \mu\text{s}$, though it was justified by the evocation of eye movements for longer exposure durations. When the 1986 standard was drafted, there was strong sentiment to do away with radiance formulations. As a result, in the 1986

and subsequent standards prior to the 2014 edition, the extended-source MPE was defined as irradiance or radiant exposure at the cornea. This was given as the product of the point-source MPE and a correction factor proportional to the diameter of the irradiated area on the retina; that is, $\text{MPE}_{(\text{TIE})} = kD$ for retinal diameters less than $\sim 1.7\ \text{mm}$.³⁰⁻³²

By definition, a point source subtends a limiting visual angle, α_{min} , of $1.5\ \text{mrad}$. The MPE for a source subtending a larger visual angle, α , is obtained by multiplying the point-source MPE by a correction factor (C_E in American National Standards Institute [ANSI] and International Commission on Non-Ionizing Radiation Protection [ICNIRP] standards, C_6 in the International Electrotechnical Commission [IEC] standard) that is a function of α . The angular or spatial distribution of the beam is the measurable parameter, but the diameter of the irradiance profile at the retina determines the damaging potential of a given quantity of energy incident on the retina. The retinal irradiance diameter D may be calculated from the source visual angle as $D = \alpha f_e$, where f_e is the effective focal length of the eye in air. For a given value of α , D is smaller in the monkey eye ($f_e = 13.5\ \text{mm}$), which is used in injury threshold studies, than in the human eye ($f_e = 17\ \text{mm}$),

TABLE 10-1

DEPENDENCE OF CORRECTION FACTOR C_E ON THE ANGULAR SUBTENSE AND THE RETINAL IRRADIANCE DIAMETER

α^*	C_E	D	C_E
$\alpha < \alpha_{\min}$	1	$D < 25 \mu\text{m}$	1
$\alpha_{\min} < \alpha < \alpha_{\max}$	α/α_{\min}	$25 \mu\text{m} < D < 1,700 \mu\text{m}$	$D/25$
$\alpha > \alpha_{\max}$	$\alpha^2/(\alpha_{\min} \times \alpha_{\max})$	$D > 1,700 \mu\text{m}$	$D^2/(25 \times 1,700)$

* $\alpha_{\min} = 1.5 \text{ mrad}$; $\alpha_{\max} = 100 \text{ mrad}$
 α : angular subtense of the source
 D: diameter (specifically, retinal irradiance diameter)

for which the standards pertain. When the intent is to compare the MPE to injury thresholds experimentally determined in the monkey eye, it is useful to express C_E as a function of D (Table 10-1, Figure 10-4). D_{\min} is the retinal irradiance diameter in the human eye calculated for the limiting visual angle, α_{\min} , and D_{\max} is the retinal irradiance diameter in the human eye calculated for $\alpha_{\max} = 100 \text{ mrad}$. In the 1986 and subsequent standards before the 2014 edition, C_E , C_6 and the MPE were directly proportional to D between 25 and 1,700 μm for the case of the human eye. (It should be noted that Table 10-1 and Figures 10-4 and 10-5 presented here are specific to the 2007 editions of the ANSI and IEC safety standards. The 2014 edition of the standards produced a different set of tables and figures. The discussion of the relationship between retinal radiant exposure and corneal radiant exposure remain relevant to the 2014 standards.)

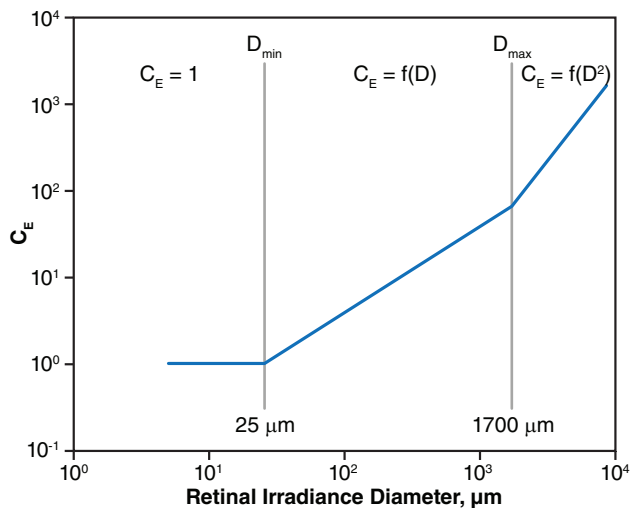


Figure 10-4. The dependence of the source-size correction factor C_E on diameter, D .

Laser exposure limits (MPEs) are defined in terms of radiant exposure or irradiance at the position of the cornea. The TIE can be derived when the MPE is multiplied by the area of a 7 mm diameter pupil, a value equivalent to the energy that enters the eye. In this sense, MPEs are defined in corneal space. The TIE is a useful measure of the dose in bioeffects studies in that the experiment is usually designed so that the laser beam incident at the cornea is smaller than the pupil, and the TIE can be and is directly measured. On the other hand, when in-vivo data are to be compared to in-vitro data or to the computed results of thermal models of laser-induced retinal

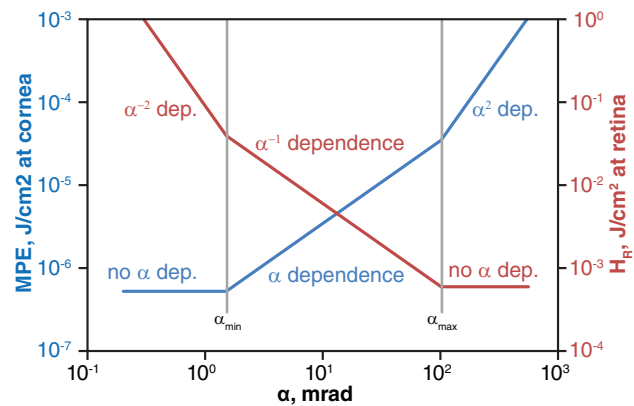


Figure 10-5. Blue: General dependence of the maximum permissible exposure (MPE) values, when specified as corneal levels, as a function of α when α_{\max} equals 100 mrad. Red: General dependence of the MPE values when specified as retinal radiant exposure, as a function of α . Because $D = f\alpha$, where f is the focal length of the eye (17 mm in the human eye), the same general dependencies of the MPE are obtained as a function of D when $D_{\max} = 1,700 \mu\text{m}$, as shown in Figure 10-4.

α : angular subtense of the source
 D : retinal irradiation diameter
 H_R : radiant exposure

injury, a more useful quantity is the retinal radiant exposure, H_R . For a perfect eye, the retinal radiant exposure is related to the incident energy at the cornea by the relationship

$$(4) \quad H_R = 4 T_\lambda \text{TIE}/(\pi D^2)$$

where T_λ is the transmission of the preretinal ocular media at the wavelength of exposure, D is the retinal image diameter assuming circular symmetry, and TIE is the energy incident at the cornea within the area of the pupil. C_E (or C_6) shows a different dependency upon α and D when the exposure is expressed as

retinal radiant exposure (Figure 10-5). Note also that while investigators can measure the angular distribution of the beam entering the eye, they cannot directly measure the irradiance diameter at the retina. The spatial distribution of energy or power at the retina (retinal spot size and irradiance profile) is a computed quantity that requires assumptions about the size and focal length of the eye, the optical quality of the eye, and the transparency of the preretinal ocular media. Large retinal area exposures are made in Maxwellian view, and α , the angle subtended by the retinal irradiance profile, is assumed equal to θ , the divergence angle of the incident beam.

HISTORICAL EMPIRICAL BASIS FOR CURRENT LASER SAFETY GUIDELINES

Experimental studies relating retinal irradiance, retinal image diameter, and retinal injury were initiated before the invention of the laser, motivated originally by the need to understand how thermal energy might be hazardous to the eyes of those who viewed nuclear detonations. Early investigators³³⁻³⁵ used high-intensity broadband light sources to induce retinal burns in rabbit and nonhuman primate retinas, and found that retinal injury thresholds varied as a function of exposure duration and retinal area. When the ruby laser became available, investigators incorporated this new light source to explore laser-induced retinal injury for pulse durations not available from broadband sources. Based on studies using a Q-switched ruby laser to irradiate large retinal areas, Ham et al concluded that 0.07 J/cm^2 at the retina was sufficient to produce retinal injury.³⁶ In experiments designed to produce small retinal spots limited only by the optics of the eye, Vassiliadis et al reported that 0.9 J/cm^2 at the retina was required to produce retinal injury.³⁷ These discordant results spurred further studies designed to better characterize the relationship between irradiated area and injury threshold.

Beatrice and Frisch¹⁶ reported data that indicated the threshold TIE varied with D for exposures to continuous wave (CW) argon lasers and Q-switched ruby lasers. Other studies^{10,38-46} conducted through the 1980s tended to support this notion (Figure 10-6). In the late 1990s, Zuclich and Lund initiated a series of studies to examine the ocular protection afforded by nonlinear devices.^{25,27,47} The studies included measuring the threshold for retinal alteration over a range of retinal irradiance diameters for exposure to 5 ns, 532 nm Nd:YAG laser irradiation and to 3 μs , 590 nm flashlamp-pumped dye laser irradiation. The data from these studies showed that the threshold TIE varied according to D^2 when D was larger than $\sim 80 \mu\text{m}$

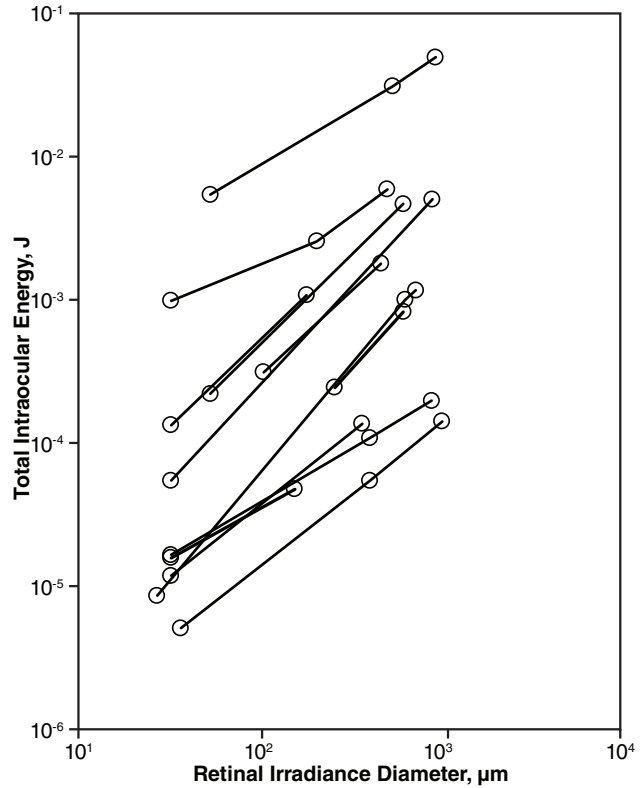
(Figure 10-7). These results were supported by the results of injury threshold studies for ultrashort lasers, which also showed that threshold TIE varied with D^2 .⁴⁸

These disparate results motivated researchers to gather all available data relating the radiant exposure required to produce retinal damage to the diameter of the irradiated area on the retina from reports of studies designed to obtain dose-response data for light irradiation of retinal tissue in vivo and in vitro. The collected data are tabulated in Tables 10-2 through 10-16. These data are expressed in units of radiant exposure (J/cm^2) at the retina as determined by equation (4). In all cases, the retinal image diameter has been computed at the point where the radiant exposure fell to $1/e$ of the peak radiant exposure, and the diameter has been adjusted to the appropriate value for a 13.5 mm focal length eye (in rhesus monkeys) or a 10 mm focal length eye (in rabbits).

Most commonly, the retinal response was observed using an ophthalmic instrument such as an ophthalmoscope, fundus camera, or slit-lamp biomicroscope. This equipment does not allow the investigator to directly observe the induced retinal alteration for near-threshold exposures, but it does allow observation of the biological or metabolic response to the induced damage (which is not instantaneous but develops over time following the exposure). Early studies used a minimum visible lesion (MVL) detectable at 5 minutes postexposure as the endpoint for determining the presence of a retinal response. Most subsequent studies reported 1-hour and/or 24-hour MVL endpoints. Some investigators employed fluorescein angiography as an indicator of retinal alteration. While the nonhuman primate is the current model of choice, many of the early studies used the rabbit as an animal model, notably studies that exposed retinal tissue to broadband radiation from a xenon lamp.

Figure 10-6. The dependence of ED_{50} on diameter, D , showing data available prior to 1990 upon which the correction factors C_E and C_6 were based before 2013.

Data sources: (1) Vassiliadis A, Rosan RC, Zweng HC. *Research on Ocular Thresholds*. Menlo Park, CA: Stanford Research Institute; 1969. <https://apps.dtic.mil/dtic/tr/fulltext/u2/700422.pdf>. Accessed December 12, 2018. (2) Beatrice ES, Frisch GD. Retinal laser damage thresholds as a function of the image diameter. *Arch Environ Health*. 1973;27:322–326. (3) Beatrice ES, Shawaluk PD. *Q-Switched Neodymium Laser Retinal Damage in Rhesus Monkey*. Philadelphia, PA: Frankford Arsenal; 1973. Report No. M73-9-1. (4) Borland RG, Brennan DH, Marshall J, Viveash JP. The role of fluorescein angiography in the detection of laser-induced damage to the retina: A threshold study for Q-switched neodymium and ruby lasers. *Exp Eye Res*. 1978;27:471–493. (5) Goldman AI, Ham WT Jr, Mueller HA. Ocular damage thresholds and mechanisms for ultrashort pulses of both visible and infrared laser radiation in the rhesus monkey. *Exp Eye Res*. 1977;24:45–56. (6) Greiss GA, Blankenstein MF, Williford GG. Ocular damage from multiple-pulse laser exposure. *Health Phys*. 1980;39:921–927. (7) Ham WT Jr, Geeraets WT, Mueller HA, Williams RC, Clarke AM, Cleary SF. Retinal burn thresholds for the helium-neon laser in the rhesus monkey. *Arch Ophthalmol*. 1970;84:797–809. (8) Lund DJ, Beatrice ES. Ocular hazards of short-pulse argon laser irradiation. *Health Phys*. 1979;36:7–11. (9) Zudlich JA, Blankenstein MF. *Additivity of Retinal Damage for Multiple Pulse Laser Exposures*. San Antonio, TX: KRUG International; 1988. US Air Force School of Aerospace Medicine Report No. TR-88-24. (10) Lund DJ. *Variation of ED_{50} With Retinal Irradiance Diameter - 850 nm Erbium Laser*. San Francisco, CA: Letterman Army Institute of Research; 1977. Laboratory Notebook U0023-G. (11) Lund DJ. *Variation of ED_{50} With Retinal Irradiance Diameter - 599 nm Flashlamp-Pumped Dye Laser*. San Francisco, CA: Letterman Army Institute of Research; 1979. Laboratory Notebook U0023-G.



Many of the datasets consisted of only two points. One was a small retinal irradiance diameter determined by the ability of the eye to focus a collimated incident beam, generally recorded at 25 to 30 μm. The second data point was at a larger irradiance diameter, between 150 and 900 μm. Due to the uncertain determination of the minimum irradiance diameter, such datasets are less reliable than those that present data for more than two image diameters.

It is difficult to draw any conclusions concerning the true relationship between the ED_{50} (the dose, expressed as TIE or H_R , having a 50% probability of causing retinal injury) and the retinal irradiance diameter by simple examination of this body of data (Figure 10-8). Each dataset can be approximated by an equation of the form:

$$(5) \quad H_R = kD^S$$

The values of S relate the retinal radiant exposure to the retinal irradiance diameter at the ED_{50} . The results of thermal model calculations show that it is an oversimplification to fit each dataset with a single

value of S^4 ; nonetheless, S so derived has utility in understanding the collected data. The value of S for a dataset is not changed when all values of D are multiplied by a constant, such as an adjustment to the eye focal length or an adjustment from the $1/e^2$ to $1/e$ diameter definition.

The value of S varies with the exposure duration (Figure 10-9). From thermal considerations, the ED_{50} is expected to be independent of the irradiance diameter ($S = 0$) for exposure durations shorter than a few microseconds when thermal conduction is not a factor. As the exposure duration increases, the value of S will decrease as thermal conduction becomes increasingly more important.

Figure 10-3 shows all datasets that include a value for the ED_{50} at or near a retinal diameter of 100 μm, as well as data for larger and smaller retinal irradiance diameters. Collectively, these datasets show an effective minimum retinal irradiance diameter below which the ED_{50} , expressed as TIE, no longer decreases as the irradiated area decreases. The effective minimum irradiance diameter is significantly larger than the minimum diameters discussed in the background section.

The analysis of the data quite clearly shows that the ED₅₀ does not simply vary with either the diameter or the area of the retinal image. In fact, the ED₅₀ varies with the irradiance diameter in a more complex manner, dependent upon the exposure duration. The

collective data called into question the pre-2013 formulation of C_E and C₆ and, to a degree, the value of α_{min}. Thermal models of laser-induced retinal injury are useful to increase understanding of the dynamics of this dependence.

PHYSICAL MODELS AND CALCULATIONS

Simple Models

Laser-induced thermal retinal damage is initiated when incident radiation is absorbed in the melanin-granule layer of the RPE. From a purely physical viewpoint, the melanin granule layer can be viewed as a thin (5–10 μm), highly absorbing layer of large lateral extent immersed in a non-absorbing media with the thermal properties of water. Radiation is incident normal to the plane of the layer. The aspect ratio of the retinal region heated by the laser is an important factor controlling the expected time–temperature history of the irradiated area. For large images, the heated portion of retina behaves as a thin disc, and any cooling occurs by heat flow perpendicular to the disc. All regions of a large, flat-topped image have equivalent exposure and dissipation opportunities, so the energy required to cause injury is proportional to the area of the image, as expressed by the safety standards for α > α_{max}. The large-image injury threshold can be described by a retinal irradiance that is independent of image size. For very small images, the diameter and thickness of the heated region become quite comparable,

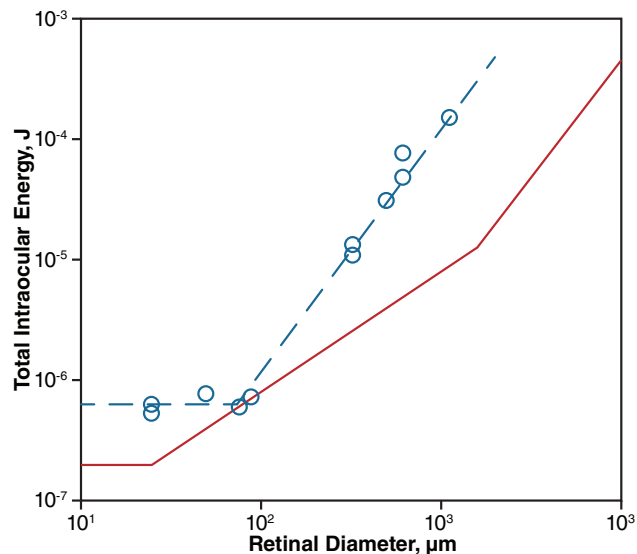


Figure 10-7. The ED₅₀ for retinal injury induced by exposure to 5 ns, 532 nm laser pulses (blue) compared to the pre-2013 maximum permissible exposure (red). Data source: Zuclich JA, Edsall PR, Lund DJ, et al. New data on the variation of laser-induced retinal damage threshold with retinal image size. *J Laser Applications*. 2008;20(2):83–88.

TABLE 10-2

TABULATION OF LASER-INDUCED RETINAL INJURY THRESHOLDS AS A FUNCTION OF THE RETINAL IRRADIANCE DIAMETER: HELIUM-CADMIUM LASER

Wavelength (nm)	Endpoint	Duration (s)	T	Retinal site	S	Retinal diameter (μm)		
						50	125	327
						Retinal radiant exposure (J/cm ²)		
442	1 h vis	1	0.4	extramacula	-1.13	177	37.2	12.6
442	48 h vis	1	0.4	extramacula	-0.96	145	31.5	12.6
442	1 h vis	5	0.4	extramacula	-1.14	611	117	39.1
442	48 h vis	5	0.4	extramacula	-1.04	591	106	39.1
442	1 h vis	16	0.4	extramacula	-1.41	—	386	99.1
442	48 h vis	16	0.4	extramacula	-0.82	—	75.1	34.1
442	48 h vis	100	0.4	extramacula	0.045	—	22.8	23.8

—: no data
 1 h vis: retinal injury detected via ophthalmoscopic examination 1 hour after exposure
 48 h vis: retinal injury detected via ophthalmoscopic examination 48 hours after exposure
 S: slope of the spot-size dependence; the retinal radiant exposure (H_R) is related to the retinal diameter (D) by the equation H_R = kD^S
 T: transmittance of the eye
 Data source: Lund DJ, Stuck BE, Edsall PR. Retinal injury thresholds for blue wavelength lasers. *Health Phys*. 2006;90(5):477–484.

TABLE 10-3
TABLATION OF LASER-INDUCED RETINAL INJURY THRESHOLDS AS A FUNCTION OF THE RETINAL IRRADIANCE DIAMETER:
ARGON LASER

Data source	Wavelength (nm)	Endpoint	Duration (s)	T	Retinal site	S	Retinal diameter (µm)								
							30	50	100	200	252	327	378	598	616
1	514	1 h vis	0.0005	0.55	extramacula	-0.64	—	—	—	—	0.273	—	—	—	0.154
1	514	1 h vis	0.012	0.55	extramacula	-0.78	—	6.16	—	—	—	—	—	—	0.875
2	488	1 h vis	0.0135	0.52	extramacula	-1.54	19.9	—	—	1.07	—	—	—	—	—
2	488	1 h vis	0.08	0.52	extramacula	-1.37	76.5	—	11.7	4.50	—	—	—	—	—
3	458	1 h vis	0.1	0.46	extramacula	-1.17	—	26.2	—	—	—	2.89	—	—	—
3	458	48 h vis	0.1	0.46	extramacula	-1.10	—	24.6	—	—	—	3.10	—	—	—
4	514	1 h vis	1.0	0.55	extramacula	-1.12	—	154	—	—	—	—	15.4	9.83	—

—: no data

1 h vis: retinal injury detected via ophthalmoscopic examination 1 hour after exposure

48 h vis: retinal injury detected via ophthalmoscopic examination 48 hours after exposure

S: slope of the spot-size dependence; the retinal radiant exposure (H_R) is related to the retinal diameter (D) by the equation $H_R = kD^S$

T: transmittance of the eye

Data sources: (1) Lund DJ, Beatrice ES. Ocular hazards of short-pulse argon laser irradiation. *Health Phys.* 1979;36:7-11. (2) Yassiliadis A, Rosan RC, Zweng HC. *Research on Ocular Thresholds*. Menlo Park, CA: Stanford Research Institute; 1969. <https://apps.dtic.mil/dtic/tr/fulltext/u2/700422.pdf>. Accessed December 12, 2018. (3) Lund DJ, Stuck BE, Edsall PR. Retinal injury thresholds for blue wavelength lasers. *Health Phys.* 2006;90(5):477-484. (4) Beatrice ES, Frisch GD. Retinal laser damage thresholds as a function of the image diameter. *Arch Environ Health.* 1973;27:322-326.

TABLE 10-4
TABLATION OF LASER-INDUCED RETINAL INJURY THRESHOLDS AS A FUNCTION OF THE RETINAL IRRADIANCE DIAMETER:
ARGON AND NEODYMIUM:YTRIUM-ALUMINUM-GARNATE (ND:YAG) LASERS

Data source	Laser	Wavelength (nm)	Endpoint	Duration (s)	T	Retinal site	S	Retinal diameter (μm)								
								20	69	136	281	500	562	1,013	1,018	2,012
1	argon	514	1 h vis	0.1	0.55	macula	-0.92	217	26.0	7.31	3.92	—	1.83	—	1.14	—
1	argon	514	1 h vis	0.1	0.55	extramacula	-0.95	294	28.1	8.10	4.06	—	1.88	—	1.18	—
1	argon	514	24 h vis	0.1	0.55	macula	-0.85	184	20.6	6.70	3.17	—	1.91	—	1.11	—
1	argon	514	24 h vis	0.1	0.55	extramacula	-0.77	215	21.9	6.44	3.56	—	2.08	—	1.31	—
2	Nd:YAG	532	1 h vis	0.1	0.57	extramacula	-0.18	—	—	—	—	2.00	—	1.51	—	1.57
2	Nd:YAG	532	24 h vis	0.1	0.57	extramacula	-0.38	—	—	—	—	2.20	—	1.74	—	1.30

—: no data

1 h vis: retinal injury detected via ophthalmoscopic examination 1 hour after exposure

24 h vis: retinal injury detected via ophthalmoscopic examination 24 hours after exposure

S: slope of the spot-size dependence; the retinal radiant exposure (H_R) is related to the retinal diameter (D) by the equation $H_R = kD^S$

T: transmittance of the eye

Data sources: (1) Lund DJ, Edsall PR, Stuck BE, Schulmeister K. Variation of laser-induced retinal injury with retinal irradiated area: 0.1 s, 514 nm exposures. *J Biomed Opt.* 2007;12(2):06180.

(2) Lund DJ. The new maximum permissible exposure: A biophysical basis. In: Barret K, ed. *Laser Safety: Tools and Training*. 2nd ed. Boca Raton: CRC Press;2014: 145–175.

TABLE 10-5
TABULATION OF LASER-INDUCED RETINAL INJURY THRESHOLDS AS A FUNCTION OF THE RETINAL IRRADIANCE DIAMETER:
NEODYMIUM:YTTTRIUM-ALUMINUM-GARNATE (ND:YAG) AND DYE LASERS

Laser	Wavelength (nm)	Endpoint	Duration (s)	T	Retinal site	S	Retinal diameter (µm)									
							22	25	76.7	77.4	88.4	289.7	326.6	614.3	1,177	1,617
Nd:YAG	532	1 h vis	7×10^9	0.57	macula	0.052	—	0.152	0.0284	—	0.011	—	0.016	0.011	0.0133	—
Nd:YAG	532	24 h vis	7×10^9	0.57	macula	0.070	—	0.075	0.0074	—	0.0069	—	0.0074	0.0095	0.0081	—
Nd:YAG	532	1 h vis	7×10^9	0.57	extramacula	-0.28	—	0.426	0.041	—	0.051	—	0.028	0.017	0.026	—
Nd:YAG	532	24 h vis	7×10^9	0.57	extramacula	-0.29	—	0.243	0.030	—	0.021	—	0.0093	0.015	0.0087	—
Dye	590	1 h vis	3×10^6	0.62	macula	0.028	1.452	—	—	0.166	—	0.068	—	—	—	0.071
Dye	590	24 h vis	3×10^6	0.62	macula	-0.18	0.555	—	—	0.156	—	0.057	—	—	—	0.042
Dye	590	1 h vis	3×10^6	0.62	extramacula	-0.12	2.267	—	—	0.266	—	0.125	—	—	—	0.103
Dye	590	24 h vis	3×10^6	0.62	extramacula	-0.13	1.582	—	—	0.223	—	0.083	—	—	—	0.066

—: no data

1 h vis: retinal injury detected via ophthalmoscopic examination 1 hour after exposure

24 h vis: retinal injury detected via ophthalmoscopic examination 24 hours after exposure

S: slope of the spot-size dependence; the retinal radiant exposure (H_R) is related to the retinal diameter (D) by the equation $H_R = kD^S$

T: transmittance of the eye

Data source: Zuclich JA, Edsall PR, Lund DJ, et al. New data on the variation of laser-induced retinal damage threshold with retinal image size. *JLA*. 2008;20(2):83–88.

TABLE 10-6
TABULATION OF LASER-INDUCED RETINAL INJURY THRESHOLDS AS A FUNCTION OF THE RETINAL IRRADIANCE DIAMETER:
HELIUM-NEON AND KRYPTON LASERS

Data source	Laser	Wavelength (nm)	Endpoint	Duration (s)	T	Retinal site	S	Retinal diameter (μm)							
								30	50	82	200	211	325	500	
1	HeNe	633	24 h vis	0.02	0.65	extramacula	-1.72	—	26.2	11.2	—	—	—	—	—
1	HeNe	633	24 h vis	0.125	0.65	extramacula	-1.15	—	97.7	38.6	—	13.0	—	—	—
1	HeNe	633	24 h vis	0.250	0.65	extramacula	-0.73	—	106	42.5	—	23.4	—	—	—
1	HeNe	633	24 h vis	0.5	0.65	extramacula	-0.75	—	197	73.2	—	37.0	26.2	—	—
1	HeNe	633	24 h vis	1.0	0.65	extramacula	-0.76	—	321	127	—	61.5	44.7	—	—
1	HeNe	633	24 h vis	3.0	0.65	extramacula	-1.19	—	—	—	—	171	104	—	—
2	Krypton	647	1 h vis	0.1	0.65	macula	-1.08	91.9	—	—	5.38	—	—	—	1.99

—: no data

1 h vis: retinal injury detected via ophthalmoscopic examination 1 hour after exposure

24 h vis: retinal injury detected via ophthalmoscopic examination 24 hours after exposure

HeNe: helium-neon

S: slope of the spot-size dependence; the retinal radiant exposure (H_R) is related to the retinal diameter (D) by the equation $H_R = kD^S$

T: transmittance of the eye

Data sources: (1) Ham WT Jr, Geeraets WT, Mueller HA, Williams RC, Clarke AM, Cleary SF. Retinal burn thresholds for the helium-neon laser in the rhesus monkey. *Arch Ophthalmol*. 1970;84:797-809. (2) Zuclich JA, Blankenstein MF. *Additivity of Retinal Damage for Multiple Pulse Laser Exposures*. San Antonio, TX: KRUG International; 1988. US Air Force School of Aerospace Medicine Report No. TR-88-24.

TABLE 10-7

TABULATION OF LASER-INDUCED RETINAL INJURY THRESHOLDS AS A FUNCTION OF THE RETINAL IRRADIANCE DIAMETER: RUBY AND DYE LASERS

Data source	Laser	Wavelength (nm)	Endpoint	Duration (s)	T	Retinal Site	S
1	Ruby	694	1 h vis	4×10^{-8}	0.67	E&M	-1.31
1	Ruby	694	1 h fluor	4×10^{-8}	0.67	E&M	-1.02
2	Ruby	694	1 h vis	3×10^{-8}	0.67	extramacula	-1.04
3	Ruby	694	1 h vis	1.7×10^{-3}	0.67	extramacula	-0.42
4	Ruby	694	5 min vis	2×10^{-3}	0.67	extramacula	-0.061
5	Dye	599	1 h vis	4×10^{-7}	0.64	extramacula	-1.02

—: no data

1 h vis: retinal injury detected via ophthalmoscopic examination 1 hour after exposure

1 h fluor: retinal injury detected via fluorescein angiography 1 hour after exposure

5 min vis: retinal injury detected via ophthalmoscopic examination 5 minutes after exposure

E&M: extramacula and macula

S: slope of spot-size dependence; the retinal radiant exposure (H_R) is related to the retinal diameter (D) by the equation $H_R = kD^S$

T: transmittance of the eye

and dissipation can occur in three dimensions. The threshold retinal irradiance is therefore higher than for the large-image value.

The extent to which heat can conduct away from the image is an important factor in the transition between the large-image and small-image extremes. According to diffusion theory, during the time, t , of the exposure, heat can conduct a distance

$$(6) \quad X = (k t / \rho C)^{0.5}$$

where k is the thermal conductivity of the tissue, ρ the density, and C the specific heat. Assuming that all these parameters exhibit values close to those of water, some $30 \mu\text{s}$ is required for heat to escape from a small ($20 \mu\text{m}$) retinal image, and some 10 s would be required for a diffusion distance of 1 mm. For exposures longer than $30 \mu\text{s}$, a significant range of D exists for which $D < X$. When, for a given pulse duration, $D < X$, then radial cooling affects the center of the irradiated spot during the pulse duration, which results in a lower temperature, and thus a higher retinal radiant exposure for threshold injury is required as compared to cases where there is no radial cooling. This produces a $1/D$ dependence of retinal injury thresholds. If, for a given pulse duration, $D > X$, then the center of the irradiated spot is not affected by radial cooling during the pulse duration, and therefore the threshold in terms of retinal

radiant exposure does not depend on the diameter, D . For pulse durations less than $\sim 30 \mu\text{s}$, this condition is met for all spot sizes. This time regime is referred to as the thermal confinement regime.

Computer Models

Computer models to estimate the temperature rise in retinal tissue were first written in efforts to understand the retinal hazard of intense broadband optical sources. Algorithms evolved to incorporate more realistic descriptions of energy deposition in retinal tissue and to include transient thermal events. Available computer models for laser-induced thermal retinal injury differ in the definition of the heat source. One definition, used by Takata, assumes absorption following Beer's law in homogeneous RPE and choroid layers and solves the heat flow equations numerically with a finite difference method.⁴⁹ Homogeneous models provide a useful description of long-exposure durations, but are less successful for sub-100 μs exposures. In reality, power absorption within the RPE is not uniform; the strongly absorbing melanin is concentrated into small ($\sim 1 \mu\text{m}$) granules called melanosomes, which are dispersed within a relatively transparent medium. On the microsecond timescale, the tissue temperatures are determined by the size and absorption of the melanosomes, and the rate of

TABLE 10-7 (continued)

TABULATION OF LASER-INDUCED RETINAL INJURY THRESHOLDS AS A FUNCTION OF THE RETINAL IRRADIANCE DIAMETER: RUBY AND DYE LASERS

Retinal diameter (μm)												
30	35	40	135	150	350	392	446	716	891	1,026	1,350	10,000
Retinal radiant exposure (J/cm^2)												
1.52	—	—	—	0.183	—	—	—	—	—	—	—	—
0.275	—	—	—	0.053	—	—	—	—	—	—	—	—
—	—	0.901	—	—	—	—	0.045	—	0.022	—	—	—
—	—	26.7	—	—	—	—	—	—	—	—	—	2.56
—	—	—	0.748	—	0.702	—	—	0.709	—	—	0.636	—
—	0.344	—	—	—	—	0.030	—	—	—	0.011	—	—

Data sources: (1) Borland RG, Brennan DH, Marshall J, Viveash JP. The role of fluorescein angiography in the detection of laser-induced damage to the retina: A threshold study for Q-switched neodymium and ruby lasers. *Exp Eye Res.* 1978;27:471–493. (2) Beatrice ES, Frisch GD. Retinal laser damage thresholds as a function of the image diameter. *Arch Environ Health.* 1973;27:322–326. (3) Vassiliadis A, Rosan RC, Peabody RR, Zweng HC, Honey RC. *Investigations of Retinal Damage Using a Q-switched Ruby Laser (AD489476)*. Menlo Park, CA: Stanford Research Institute; 1966. (4) Allen RG, Bruce WR, Kay KR, et al. *Research on Ocular Effects Produced by Thermal Radiation*. Brooks Air Force Base, TX: US Air Force; 1967. Final Report AF41(609)-3099, AD659146. (5) Lund DJ. *Variation of ED₅₀ With Retinal Irradiance Diameter - 599 nm Flashlamp-Pumped Dye Laser*. San Francisco, CA: Letterman Army Institute of Research; 1979. Laboratory Notebook U0023-G.

conduction from the granules into the surrounding tissue. For short exposures, the temperature proximal to the melanosomes rises considerably higher than a continuum model would predict.

Granule models were developed to deal with this shortcoming.⁵⁰⁻⁵⁴ Power absorption is assumed to be confined to the granules, and heat subsequently diffuses into the surrounding tissue, where criteria are applied to predict whether cell death will occur. In recent years, the most widely used version has been that of Thompson and Gerstman,⁵⁴ which builds on several of the earlier models. Theirs is a single-granule model, in the sense that a single solution of the heat diffusion equation is used for all granules. Provided that the incident laser power has a flat-topped temporal profile of finite duration, then an analytical solution can be found for the time-dependent temperature distribution $T_i(r,t)$ at radius r from the i^{th} granule. The temperature distribution around an array of granules is calculated by linear superposition of the individual solutions, taking into account the relative positions of the individual granules. Apart from this superposition process, thermal interaction between different granules is neglected. The model can accommodate laser images of different sizes and profiles by scaling the single solution $T_i(r,t)$ according to the local irradiance at the location of each granule. The Thompson-Gerstman model successfully describes the dependence of

ED₅₀ on exposure duration across a very wide range. However, it is currently a thermal damage model only and cannot account for microcavitation bubbles, which appear to result in lower damage levels in comparison to purely thermally induced damage. In-vitro data show that microcavitation bubble formation leads to lower damage thresholds for exposures shorter than $\sim 10 \mu\text{s}$.^{6,7} When optical and thermal properties are set to equivalent values, both the Takata model⁴⁹ and the Thompson-Gerstman model result in identical thresholds for pulse durations longer than $\sim 10 \mu\text{s}$.⁵⁵

Current models include the Arrhenius integral to determine an endpoint for damage.⁵⁶ The Arrhenius model attributes cell death to a hypothetical chemical reaction with a temperature-dependent rate given by

$$(7) \quad \int A \exp\left(-\frac{E}{RT(r,t)}\right) dt = 1$$

where E is the activation energy of the reaction, R is the molar gas constant, and A is a multiplying rate constant with the dimensions of inverse time. The progress of this reaction is integrated over the entire heating cycle induced by the laser exposure, and the injury threshold is determined by the minimum incident laser energy that makes the time-integrated reaction equal to unity at some point within a cell, or within a certain given area comparable to the concept of MVL. This damage

TABLE 10-8
TABULATION OF LASER-INDUCED RETINAL INJURY THRESHOLDS AS A FUNCTION OF THE RETINAL IRRADIANCE DIAMETER:
NEODYMIUM:YTRITIUM-ALUMINUM-GARNATE (ND:YAG), ND:GLASS, AND ERBIUM:YAG LASERS

Data source	Laser	Wavelength (nm)	Endpoint	Duration (s)	T	Retinal site	Retinal diameter (µm)							
							25	30	60	100	175	362	460	875
1	Nd:YAG	1,064	1 h vis	1.5×10^{-8}	0.57	extramacula	-0.57	-	8.65	2.30	-	-	0.623	-
2	Nd:YAG	1,064	1 h vis	1.6×10^{-8}	0.57	extramacula	-0.66	-	4.47	-	-	-	-	0.485
2	Nd:YAG	1,064	24 h vis	1.6×10^{-8}	0.57	extramacula	-0.68	-	3.60	-	-	-	-	0.359
3	Nd:Glass	1,059	1 h vis	1.5×10^{-8}	0.57	E&M	-0.81	-	10.9	-	-	2.59	-	-
3	Nd:Glass	1,059	1 h fluor	1.5×10^{-8}	0.57	E&M	-0.80	-	3.79	-	-	0.796	-	-
4	Erbium:YAG	850	1 h vis	1.8×10^{-7}	0.72	extramacula	-1.11	1.79	-	-	-	-	0.092	-

--: no data

1 h vis: retinal injury detected via ophthalmoscopic examination 1 hour after exposure

1 h fluor: retinal injury detected via fluorescein angiography 1 hour after exposure

24 h vis: retinal injury detected via ophthalmoscopic examination 24 hours after exposure

E&M: extramacular and macular

S: slope of the spot-size dependence; the retinal radiant exposure (HR) is related to the retinal diameter (D) by the equation $H_R = kD^S$

T: transmittance of the eye

Data sources: (1) Beatrice ES, Shawaluk PD. *Q-Switched Neodymium Laser Retinal Damage in Rhesus Monkey*. Philadelphia, PA: Frankford Arsenal; 1973. Report No. M73-9-1. (2) Greiss GA, Blankenstein MF, Williford GG. Ocular damage from multiple-pulse laser exposure. *Health Phys*. 1980;39:921-927. (3) Borland RC, Brennan DH, Marshall J, Viveash JP. The role of fluorescein angiography in the detection of laser-induced damage to the retina: A threshold study for Q-switched neodymium and ruby lasers. *Exp Eye Res*. 1978;27:471-493. (4) Lund DJ. *Variation of ED₅₀ With Retinal Irradiance Diameter - 850 nm Erbium Laser*. San Francisco, CA: Letterman Army Institute of Research; 1977. Laboratory Notebook U0023-G.

TABLE 10-9
TABLATION OF LASER-INDUCED RETINAL INJURY THRESHOLDS AS A FUNCTION OF THE RETINAL IRRADIANCE DIAMETER:
TITANIUM-SAPPHIRE (Ti:SAPH) AND NEODYMIUM:YTRITIUM-ALUMINUM-GARNATE (Nd:YAG) LASERS

Data source	Laser	Wavelength (nm)	Endpoint	Duration (s)	T	Retinal site	S	Retinal diameter (μm)									
								30	48	70	102	224	304	378	445	512	804
1	Ti:Saph	1,060	1 h vis	1.5×10^{13}	0.57	macula	-0.43	—	0.0724	0.0267	0.0223	0.0240	—	0.0194	—	—	0.0091
1	Ti:Saph	1,060	24 h vis	1.5×10^{13}	0.57	macula	-0.41	—	0.0315	0.0148	0.0146	0.0104	—	0.0100	—	—	0.0061
1	Ti:Saph	1,060	1 h fluor	1.5×10^{13}	0.57	macula	-0.26	—	—	0.227	0.0384	0.0146	—	0.0163	—	—	0.0212
1	Ti:Saph	1,060	24 h fluor	1.5×10^{13}	0.57	macula	-0.37	—	—	0.181	0.0516	0.0175	—	0.0179	—	—	0.0230
2	Nd:YAG	1,065	24 h vis	3×10^{11}	0.57	macula	-0.18	0.702	—	—	—	1.19	—	0.373	0.328	—	—

—: no data

1 h vis: retinal injury detected via ophthalmoscopic examination 1 hour after exposure

1 h fluor: retinal injury detected via fluorescein angiography 1 hour after exposure

24 h vis: retinal injury detected via ophthalmoscopic examination 24 hours after exposure

24 h fluor: retinal injury detected via fluorescein angiography 24 hours after exposure

E&M: extramacular and macular

S: slope of the spot-size dependence; the retinal radiant exposure (HR) is related to the retinal diameter (D) by the equation $H_r = kD^S$

T: transmittance of the eye

Data sources: (1) Cain CP, Toth CA, Noojin GD, et al. Visible lesion threshold dependence on retinal spot size for femtosecond laser pulses in the primate eye. *JLA*. 2001;13(3):125–131.
 (2) Goldman AL, Ham WTJ, Mueller HA. Ocular damage thresholds and mechanisms for ultrashort pulses of both visible and infrared laser radiation in the rhesus monkey. *Exp Eye Res*. 1977;24:45–56.

TABLE 10-10

TABULATION OF LASER-INDUCED RETINAL INJURY THRESHOLDS AS A FUNCTION OF THE RETINAL IRRADIANCE DIAMETER IN THE RABBIT*: RUBY, DYE, AND HELIUM-NEON LASER

Data source	Laser	Wavelength (nm)	Endpoint	Duration (s)	T	S
1	Ruby	694	5 min vis	1.6×10^{-8}	0.67	-1.95
2	Ruby	694	5 min vis	3×10^{-8}	0.67	-0.73
3	Dye	593	15 min vis	6×10^{-7}	0.63	-1.78
3	Dye	593	15 min fluor	6×10^{-7}	0.63	-1.15
3	Dye	593	24 h vis	6×10^{-7}	0.63	-1.21
3	Dye	593	24 h fluor	6×10^{-7}	0.63	-1.40
4	HeNe	633	1 h vis	10	0.65	-1.56
4	HeNe	633	24 h vis	10	0.65	-1.56

*Retinal site not applicable in rabbits

—: no data

5 min vis: retinal injury detected via ophthalmoscopic examination 5 minutes after exposure

15 min vis: retinal injury detected via ophthalmoscopic examination 15 minutes after exposure

1 h vis: retinal injury detected via ophthalmoscopic examination 1 hour after exposure

1 h fluor: retinal injury detected via fluorescein angiography 1 hour after exposure

24 h vis: retinal injury detected via ophthalmoscopic examination 24 hours after exposure

24 h fluor: retinal injury detected via fluorescein angiography 24 hours after exposure

HeNe: helium-neon

S: slope of the spot-size dependence. The retinal radiant exposure (H_R) is related to the retinal diameter (D) by the equation $H_R = kD^S$

T: transmittance of the eye

criterion takes some account of both the amplitude and the duration of the temperature excursion, and provides a basis for modeling of both long and short exposures.

Model Results

Both the homogeneous absorber model and the granule model have been used to predict the spot-size dependence of the injury threshold.^{55,57,58} The computational results obtained by Schulmeister et al⁴ are of special significance for two reasons. First, they present an exhaustive examination of the dependence of computed retinal injury thresholds upon retinal irradiance diameter over a range from 30 μm to 2,000 μm , and upon exposure duration over the range from 1 μs to 1 s. Second, the computational results were directly compared to and validated by injury thresholds resulting from laser exposure of bovine retinal explants in vitro over a range of irradiance diameters from 23 μm to 2,000 μm and exposure durations from 100 μs to 2 s.⁴ Table 10-16 lists these in-vitro retinal injury thresholds. Figure 10-10 shows the in-vitro injury threshold data and computational results obtained with the Thompson-Gerstman model. The thermal model results were obtained by providing

a retinal irradiance diameter and radiant exposure profile as input data and allowing the program to obtain a solution for the threshold radiant exposure. A top-hat (constant irradiance) beam profile was assumed, as well as a square-wave temporal pulse shape. The computed thresholds, expressed as retinal radiant exposure, vary inversely to the diameter of the irradiated area for small spots and are independent of the irradiance diameter for large spots. The range of transition between the two zones in terms of retinal spot diameter is a function of the exposure duration. A breakpoint (Bp) can be obtained as the point of intersection of lines projected from the two zones (Figures 10-10 and 10-11).

Figure 10-12 compares the thermal model predictions (optimized to model rhesus monkey macular thresholds for a wavelength of 532 nm) to the data for those exposure durations where data are available. Considering that part of the data represents incoherent radiation exposures in rabbit eyes, the model predicts the trend of the data reasonably well for exposure durations as short as 3 μs . Laser-induced retinal injury for exposure durations shorter than a few microseconds does not result from thermal denaturation of tissue, but rather is induced by superheating the melanosomes, leading to bubble

TABLE 10-10 (continued)

TABULATION OF LASER-INDUCED RETINAL INJURY THRESHOLDS AS A FUNCTION OF THE RETINAL IRRADIANCE DIAMETER IN THE RABBIT*: RUBY, DYE, AND HELIUM-NEON LASER

8	Retinal diameter (µm)													
	30	50	70	100	150	180	260	286	350	400	520	572	800	1,000
Retinal radiant exposure (J/cm ²)														
483	—	11.1	—	—	2.32	—	—	—	—	0.260	—	—	0.050	—
—	—	0.409	—	0.341	—	0.234	—	—	0.153	—	0.0347	—	0.0493	0.0606
—	—	—	—	—	—	—	—	0.0862	—	—	—	0.0251	—	—
—	0.455	—	0.121	—	—	—	—	0.0271	—	—	—	0.0104	—	—
—	0.677	—	—	—	—	—	—	0.0459	—	—	—	0.0189	—	—
—	0.891	—	—	—	—	—	—	0.0399	—	—	—	0.0140	—	—
—	—	—	—	504	—	—	178	—	—	—	—	—	20	—
—	—	—	—	471	—	—	166	—	—	—	—	—	20.2	—

Data sources: (1) Bergqvist T, Kleman B, Tengroth B. Retinal lesions produced by Q-switched lasers. *Acta Ophth.* 1966;44:853–863. (2) Ham WT Jr, Geeraets WT, Williams RC, Guerry D III, Mueller HA. Laser radiation protection. In: *Proceedings of the First International Congress of Radiation Protection*. New York, NY: Pergamon Press; 1968:933–943. (3) Courant D, Court L, Abadie B, Brouillet B. Retinal damage thresholds from single-pulse laser exposures in the visible spectrum. *Health Phys.* 1989;56(5):637–642. (4) Davis TP, Mautner WJ. *Helium Neon Laser Effects on the Eye*. Los Angeles, CA: EG&G Inc, Santa Monica Division; 1969. Report C10659233.

TABLE 10-11

TABULATION OF INCOHERENT RADIATION-INDUCED RETINAL INJURY THRESHOLDS AS A FUNCTION OF THE RETINAL IRRADIANCE DIAMETER IN THE RABBIT*: XENON ARC LAMP, 1967 STUDY

Wavelength (nm)	Endpoint	Duration (s)	T	S	Retinal diameter (µm)									
					53	67	90	180	260	540	1,080			
					Retinal radiant exposure (J/cm ²)									
400–900	5 min vis	0.00017	0.65	-0.17	—	—	0.686	0.457	0.383	0.423	0.415			
400–900	5 min vis	0.0004	0.65	-0.47	—	—	1.35	0.845	0.615	0.533	0.403			
400–900	5 min vis	0.001	0.65	-0.46	3.82	—	1.97	—	1.02	0.706	0.642			
400–900	5 min vis	0.004	0.65	-0.12	5.40	5.19	5.28	4.67	—	—	—			
400–900	5 min vis	0.01	0.65	-0.37	8.92	7.85	7.27	2.30	1.75	1.53	1.13			
400–900	5 min vis	0.02	0.65	-1.53	15.8	11.1	—	—	—	—	—			
400–900	5 min vis	0.04	0.65	-0.59	22.9	15.4	15.8	4.45	3.89	1.93	1.69			
400–900	5 min vis	0.1	0.65	-0.76	40.3	29.7	29.3	9.32	7.12	3.21	2.55			
400–900	5 min vis	0.25	0.65	-0.97	84.0	67.2	60.4	22.2	13.0	5.74	3.95			
400–900	5 min vis	1.0	0.65	-1.00	—	—	209	68.4	49.2	20.7	11.9			
400–900	5 min vis	4.0	0.65	-1.07	—	—	783	242	175	68.9	37.9			
400–900	5 min vis	10	0.65	-1.16	—	—	1,900	578	409	151	76.1			

*Retinal site not applicable in rabbits.

—: no data

5 min vis: retinal injury detected via ophthalmoscopic examination 5 minutes after exposure

S: slope of the spot-size dependence; the retinal radiant exposure (H_R) is related to the retinal diameter (D) by the equation $H_R = kD^S$

T: transmittance of the eye

Data source: Allen RG, Bruce WR, Kay KR, et al. *Research on Ocular Effects Produced by Thermal Radiation*. Brooks Air Force Base, TX: US Air Force; 1967. Final Report AF41(609)-3099, AD659146.

TABLE 10-12

TABULATION OF INCOHERENT RADIATION-INDUCED RETINAL INJURY THRESHOLDS AS A FUNCTION OF THE RETINAL IRRADIANCE DIAMETER IN NONHUMAN PRIMATES: XENON ARC LAMP

Wavelength (nm)	Endpoint	Duration (s)	T	Retinal site	S	Retinal diameter (µm)				
						110	220	310	640	1,300
						Retinal radiant exposure (J/cm ²)				
400-900	5 min vis	0.004	0.65	E&M	0.15	—	1.35	1.00	1.47	—
400-900	5 min vis	0.01	0.65	E&M	-0.49	7.40	2.95	1.73	3.31	—
400-900	5 min vis	0.02	0.65	E&M	-0.31	11.2	5.26	3.38	4.84	4.30
400-900	5 min vis	0.04	0.65	E&M	-0.30	13.0	7.33	4.07	5.00	5.81
400-900	5 min vis	0.1	0.65	E&M	-0.63	33.3	12.9	9.20	6.83	6.60
400-900	5 min vis	0.25	0.65	E&M	-0.74	76.8	24.6	12.3	14.1	10.2

—: no data

5 min vis: retinal injury detected via ophthalmoscopic examination 5 minutes after exposure

E&M: extramacular and macular

S: slope of the spot-size dependence; the retinal radiant exposure (H_R) is related to the retinal diameter (D) by the equation $H_R = kD^S$

T: transmittance of the eye

Data source: Allen RG, Bruce WR, Kay KR, et al. *Research on Ocular Effects Produced by Thermal Radiation*. Brooks Air Force Base, TX: US Air Force; 1967. Final Report AF41(609)-3099, AD659146.

TABLE 10-13

TABULATION OF INCOHERENT RADIATION-INDUCED RETINAL INJURY THRESHOLDS AS A FUNCTION OF THE RETINAL IRRADIANCE DIAMETER IN THE RABBIT*: XENON ARC LAMP, 1958 STUDY

Wavelength (nm)	Endpoint	Duration (s)	T	S	Retinal diameter (µm)						
					180	240	360	710	710	1,100	1,100
					Retinal radiant exposure (J/cm ²)						
400-900	5 min vis	0.025 (.02-.03)	0.65	-0.74	—	—	7.41	5.95	—	3.71	3.13
400-900	5 min vis	0.05 (.027-.057)	0.65	-0.62	—	11.8	—	7.72	6.29	4.25	—
400-900	5 min vis	0.1 (.09-.11)	0.65	-0.96	—	20.6	—	9.18	—	4.45	—
400-900	5 min vis	0.19 (.14-24)	0.65	-1.25	52.4	41.5	—	9.45	—	5.92	—

*Retinal site not applicable in rabbits.

—: no data

5 min vis: retinal injury detected via ophthalmoscopic examination 5 minutes after exposure

S: slope of the spot-size dependence; the retinal radiant exposure (H_R) is related to the retinal diameter (D) by the equation $H_R = kD^S$

T: transmittance of the eye

Data source: Ham WT Jr, Wisenger H, Schmidt FH, et al. Flash burns in the rabbit retina as a means of evaluating the retinal hazard from nuclear weapons. *Am J Ophthalmol*. 1958;46:700-723.

TABLE 10-14

TABULATION OF INCOHERENT RADIATION-INDUCED RETINAL INJURY THRESHOLDS AS A FUNCTION OF THE RETINAL IRRADIANCE DIAMETER IN THE RABBIT*: XENON ARC LAMP, 1962 STUDY

Wavelength (nm)	Endpoint	Duration (s)	T	S	Retinal diameter (μm)			
					700	1,000	2,000	4,000
400-900	5 min vis	0.023	0.65	—	—	—	—	2.67
400-900	5 min vis	0.027	0.65	—	—	—	1.90	—
400-900	5 min vis	0.084	0.65	—	—	2.445	—	—
400-900	5 min vis	0.111	0.65	—	—	2.69	—	—
400-900	5 min vis	0.116	0.65	—	—	—	2.96	—
400-900	5 min vis	0.151	0.65	—	—	—	2.80	—
400-900	5 min vis	0.43	0.65	—	5.97	—	—	—
400-900	5 min vis	0.441	0.65	—	6.34	—	—	—
400-900	5 min vis	0.466	0.65	—	6.47	—	—	—
400-900	5 min vis	0.53	0.65	—	6.91	—	—	—
400-900	NA	0.1 (projected) [†]	NA	0.12	3.24	2.61	2.83	3.78

*Retinal site not applicable in rabbits.

[†]Values in this row were projected from values in previous rows on the assumption that the ED_{50} varies proportionally to $t^{3/4}$, where t is the exposure duration.

—: no data

5 min vis: retinal injury detected via ophthalmoscopic examination 5 minutes after exposure

NA: not applicable

S: slope of the spot-size dependence; the retinal radiant exposure (H_R) is related to the retinal diameter (D) by the equation $H_R = kD^S$

T: transmittance of the eye

Data source: Jacobson JH, Cooper B, Najac HW. Jacobson JH, Cooper B, Najac HW. *Effects of Thermal Energy on Retinal Function*. Wright-Patterson Air Force Base, OH: Aerospace Medical Division; 1962. Air Force Systems Command Report AMRL-TDR-62-96.

TABLE 10-15

TABULATION OF LASER-INDUCED INJURY THRESHOLDS IN RETINAL EXPLANTS AS A FUNCTION OF THE RETINAL IRRADIANCE DIAMETER: TITANIUM:SAPPHIRE (TI:SAPH), RUBY, AND NEODYMIUM:YTTRIUM-ALUMINUM-GARNATE (ND:YAG) LASERS

Data source	Laser	Wavelength (nm)	Endpoint	Duration (s)	S	Retinal diameter (μm)							
						20	40	44	86	100	135	200	273
1	Nd:YAG	532	Cell death	1×10^{-10}	0	0.045	0.042	—	—	0.041	—	0.045	—
2	Ruby	694	Cell death	2.85×10^{-8}	0	0.114	—	—	—	—	0.114	—	—
3	Ti:Saph	1,055	Cell death	7×10^{-9}	-0.52	—	—	2.74	1.83	—	—	—	1.05

—: no data

S: slope of the spot-size dependence; the retinal radiant exposure (H_R) is related to the retinal diameter (D) by the equation $H_R = kD^S$

Data sources: (1) Roegen J, Lin CP. Photomechanical effects - experimental studies of pigment granule absorption, cavitation and cell damage. *SPIE*. 2000;3902:35-40. (2) King RG, Geeraets WT. The effect of Q-switched ruby laser on retinal pigment epithelium in vitro. *Acta Ophthalmol*. 1968;46:617-631. (3) Mills BM, Connor TM, Foltz MS, et al. Microcavitation and spot size dependence for damage of artificially pigmented hTERT-RPE1 cells. *SPIE*. 2004;5319:217-223.

TABLE 10-16

TABULATION OF LASER-INDUCED INJURY THRESHOLDS IN RETINAL EXPLANTS AS A FUNCTION OF THE RETINAL IRRADIANCE DIAMETER: NEODYMIUM:YTTTRIUM-ALUMINUM-GARNATE (ND:YAG) LASER

Wavelength (nm)	Endpoint	Duration (s)	Retinal diameter (μm)								
			23	73	120	200	288	549	894	1,508	2,000
			Retinal radiant exposure (J/cm ²)								
532	Cell death	0.0001	0.789	0.293	0.284	0.319	0.301	—	—	—	—
532	Cell death	0.001	2.03	0.719	0.747	—	0.700	0.712	—	—	—
532	Cell death	0.01	11.1	3.51	2.13	—	1.86	2.00	1.56	1.62	—
532	Cell death	0.1	90.4	19.3	12.0	—	6.24	4.63	4.50	4.05	—
532	Cell death	0.655	439	117	68.6	—	24.9	—	11.1	—	8.72
532	Cell death	2.0	—	—	187	—	—	41.8	—	—	22.0

—: no data

Data source: Schulmeister K, Husinski J, Seiser B, et al. Ex vivo and computer model study on retinal thermal laser-induced damage in the visible wavelength range. *J Biomed Opt.* 2008;13(5):054038.

formation, followed by cell death. As noted, current thermal models are not adequate to predict tissue injury based on these interaction mechanisms.

Variations to Fit the Small Spots

Kennedy et al attempted to fit the thermal models to the available data for spot sizes less than 100 μm by adjusting the input parameters.⁵⁹ They found that the granule model alone was unable to account for the

full extent of the experimentally observed departure of ED₅₀ (TIE) from a square-law dependence for small image sizes using plausible parameter values. In this study, measures that would improve the quality of the fit included the following: (1) Assignment of greater thickness to the RPE layer within which the laser energy is absorbed. This thickness controls the value of the image diameter where heat conduction out of the layer changes from a 1-dimensional process to a 3-dimensional process, and this is what ultimately

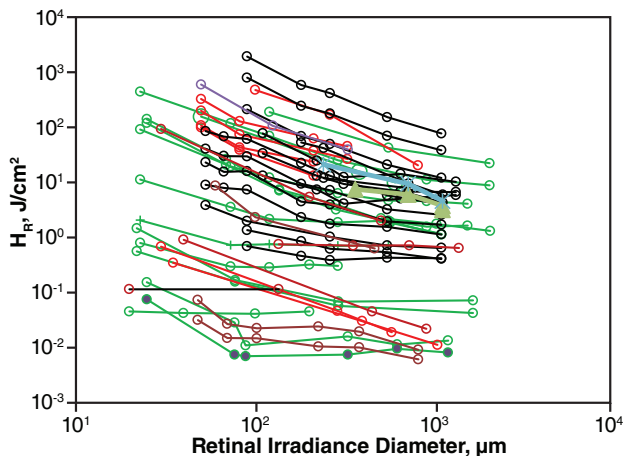


Figure 10-8. The variation of ED₅₀ for laser-induced retinal injury (retinal radiant exposure, J/cm²) with the retinal irradiance diameter. These data, tabulated in Tables 10-2 to 10-16, included exposure durations from femtoseconds to kiloseconds and wavelengths from 400 nm to 1,100 nm. H_R: radiant exposure

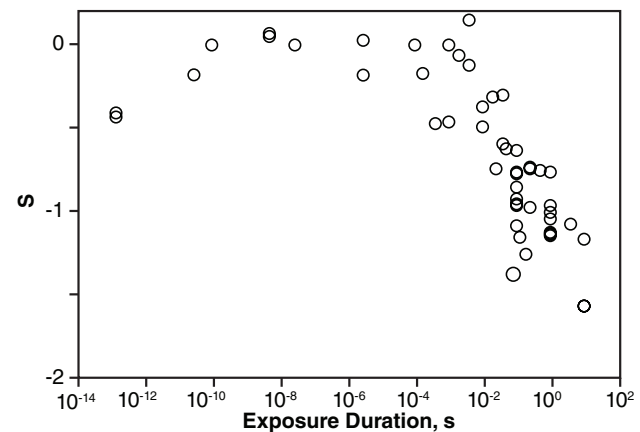


Figure 10-9. The exposure duration dependence of the slope, S, of ED₅₀ versus diameter, D. Each point is the value S obtained by fitting the data of a single line in Figure 10-8 to an equation of the form

$$H_R = kD^S$$

where H_R = radiant exposure and k is a constant relating H_R at D = D₀ to the value D₀.

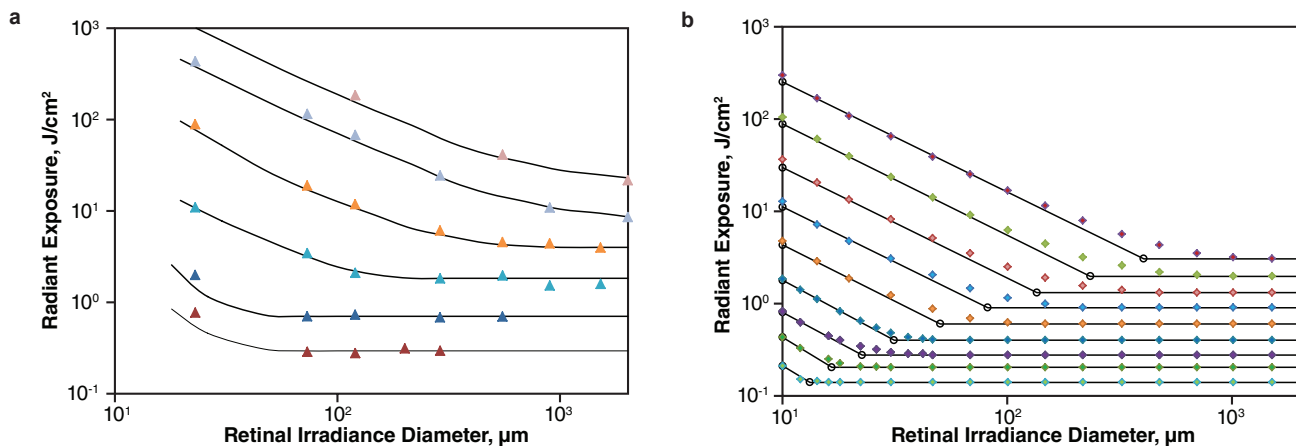


Figure 10-10. (a) Damage threshold values for bovine in-vitro samples plotted as retinal radial exposure for exposure durations of 0.1, 1, 10, 100, 655, and 2,000 ms (starting at the bottom) (b) Computer model threshold data with tighter spacing of data (exposure durations of 0.01, 0.1, 0.315, 1.0, 3.16, 10, 31.6, 100, and 316 ms, starting at bottom) and larger ranges than the experimental threshold data. A breakpoint, B_p, is obtained from the projected points of intersection. Data source: Schulmeister K, Husinski J, Seiser B, et al. Ex vivo and computer model study on retinal thermal laser-induced damage in the visible wavelength range. *J Biomed Opt.* 2008;13(5):054038.

controls the dependence of ED₅₀ on image size. (2) Assignment of larger diameters to the smallest of the retinal images to account for the possibility that the irradiated diameter in the rhesus monkey eye was larger than expected. The smallest images would need to be assigned diameters of at least 30 to 40 µm.

Schulmeister et al.^{4,60} performed thermal model calculations based on three possible interpretations for the observed spot size dependence for small spots. Under the first interpretation, lesions can only be detected ophthalmoscopically if they have some minimum size that might be larger than previously assumed. To explain the experimental spot size dependence, the MVL dimension would need to have a diameter of ~70 µm. The model can account for this by determining the damage threshold with the criterion that an area with a diameter of at least 70 µm must have values of the damage integral larger than 1. The experimentally determined threshold then constitutes a super-threshold compared to the real threshold for an undetectable smaller lesion. Alternatively, an MVL is commonly described as a subtle darkening of the exposure site, which may plausibly result from changes in the essentially transparent sensory retina overlying the RPE. It is also plausible that the threshold for a visible change in the sensory retina might differ from the threshold for a visible change in the RPE. This can be accounted for in the model by evaluating the integral damage in the sensory retina anterior to the RPE layer. A spot-size dependence trend akin to the one seen in the experimental data is found. Or,

finally, a larger than expected irradiance diameter at the RPE could be caused by intra-retinal scattering in the sensory retina before the radiation reaches the RPE.

Till et al proposed a damage model that describes the injury process as a combination of thermal and nonthermal processes.⁵⁸ Their model differs fundamentally from the longstanding Arrhenius model in that only the initial insult to the tissue is described

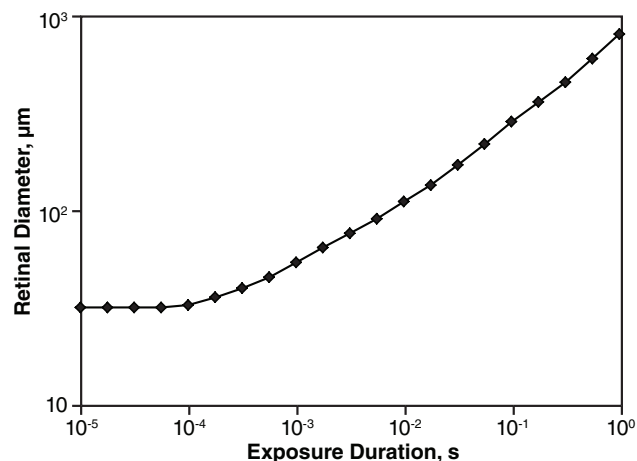


Figure 10-11. The breakpoint, B_p, as a function of exposure duration. Data source: Schulmeister K, Husinski J, Seiser B, et al. Ex vivo and computer model study on retinal thermal laser-induced damage in the visible wavelength range. *J Biomed Opt.* 2008;13(5):054038.

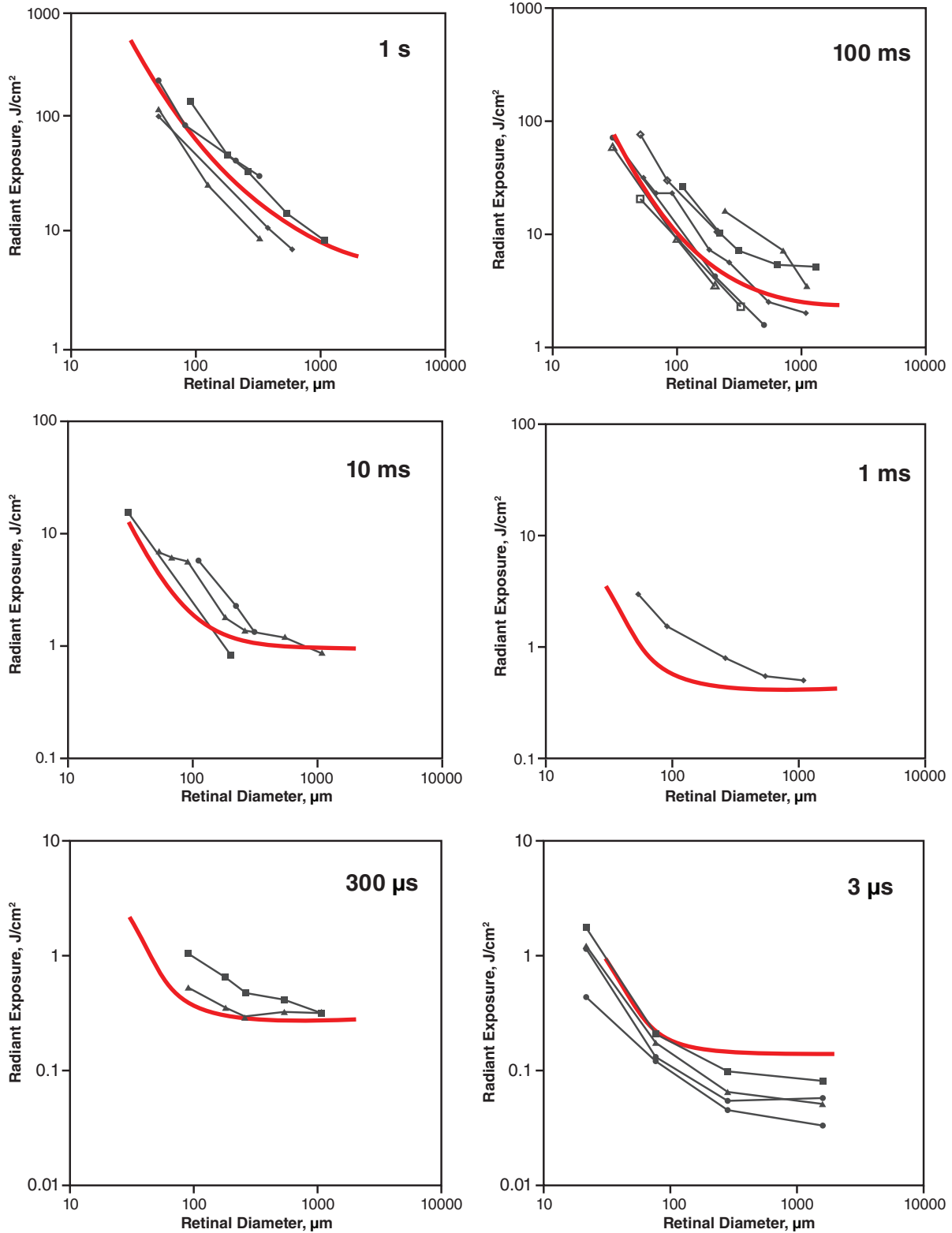


Figure 10-12. A comparison of the thermal model results optimized for macular rhesus thresholds for 530 nm exposures to the data for those exposure durations where data were available in Tables 10-2 through 10-16. The red line represents the thermal model calculations. The data include thresholds for extramacular exposures in the rhesus eye and incoherent radiation exposures in the rabbit eye.

by a thermal process; the formation of a lesion is controlled by cell chemistry that occurs during the minutes and hours following laser exposure. Typically, in-vivo MVLs are detected ophthalmoscopically an hour or more after exposure. On the other hand, in-vitro studies with eye explants and viability staining indicate that RPE cells die immediately following laser exposure.^{60,61} In-vitro threshold values in the pulse duration range of 100 μ s to 2 s and spot sizes in the intermediate range compare very well with injury thresholds predicted by the thermal model based on the Arrhenius integral, using the same model parameters that also fit the nonhuman primate thresholds.⁴ This model was later refined using a finite element method and validated against available rhesus monkey threshold data.⁶²

Images With Complex Profiles

Animal experiments usually produce either a top-hat or a Gaussian beam profile at the retina. For these two profiles, the parameter “diameter” is relatively well defined. A top-hat profile has a clearly defined diameter. If the diameter of a Gaussian beam profile is defined at the points where the irradiance drops to $1/e$ times the peak irradiance, then the Gaussian profile has the same peak radiant exposure as a top-hat profile with the same diameter. The ED_{50} for top-hat and Gaussian beams are the same to within a factor of 1.3, depending on the pulse duration and spot size (personal communication from Mathieu Jean, Seibersdorf Laboratories, Seibersdorf, Austria, ca 2010). However, such well-behaved retinal irradiance profiles are not always realized in real-world exposure scenarios. Thus, it is useful to define the “diameter” of the retinal irradiance profile in a general way. The ED_{50} s for thermally induced damage of the retina and the MPEs scale with a diameter. However, this

diameter should not be understood in the sense of an optical diameter, but rather as a thermally effective parameter, a scaling factor for the thermal damage threshold. In this sense, the ideal diameter definition for a given arbitrary retinal irradiance profile would produce a thermally effective diameter, D_{eff} such that the damage threshold is the same as the threshold for a top-hat profile with the diameter D_{eff} . This would ensure that the MPE, when given as the small spot value with a multiplication factor containing D_{eff} would scale in the same way as the thresholds scale. Currently, no criterion yields accurate results for all profiles and pulse durations.

Approaches to the development of such a criterion have been suggested. Schulmeister⁵⁵ proposed extending the multiple source criteria of IEC 60825-1 to include general irradiance profiles. This technique examines the entire profile to find the sub-area of the profile having the most restrictive combination ratio of (power within an area)/(diameter of area). In practice, this technique lends itself to the evaluation of digital camera images in which the signal of each pixel is characteristic of the local irradiance. This criterion was adopted in the second edition of the IEC standard.³²

A related semi-empirical technique based on the concept of encircled energy provides a means to adapt the available injury threshold data (for flat-topped disc images) to describe images with complex profiles, provided they are circularly symmetric.⁶³ The technique compares the energy contained in circular portions of the complex image (the “encircled energy”) against the experimentally determined ED_{50} energy for a disc-shaped image of equal diameter. Another related approach is taken by Riehl et al,⁶⁴ who propose a technique wherein the retinal irradiation distribution is convoluted by a circular filter and the maximum of the convolution is compared to the MPE for the diameter of the filter.

DISCUSSION AND CONCLUSIONS

The preceding analysis of the relationship of laser-induced retinal injury to the diameter of the irradiated area on the retina as evidenced by bioeffects data and thermal models leads to the conclusion that the formulation of C_E and C_6 in the 2007 editions of the guidelines^{30,32} was not accurate. The empirical and thermal models suggest that the value of α_{max} should vary with exposure duration, and the in-vivo bioeffects data challenge the value of α_{min} .

It was shown that the thermal model, the explant in-vitro data, and the in-vivo data all support definition of a breakpoint, B_p , separating the small-spot regime from the large-spot regime that varies with exposure

duration. It is recognized that the transition from small-to large-spot regime is gradual rather than abrupt as implied by a breakpoint; still, the defined B_p is useful. The B_p is the value of D that separates the zone in which the ED_{50} , expressed as $H_{R'}$, varies as D^{-1} from the zone in which the ED_{50} is independent of D . In terms of the TIE, this is equivalent to the point separating the zone in which the ED_{50} varies with D from the zone in which the ED_{50} varies with D^2 . Because D is proportional to α , this is also the definition of α_{max} . Thus, the observation that B_p varies with the exposure duration is an observation that the value of α_{max} should also vary as a function of the exposure duration. Based on the observed form of

TABLE 10-17
PROPOSED TIME DEPENDENCE OF THE
MAXIMUM ANGULAR SUBTENSE*

t	α_{\max} (mrad)
< 625 μ s	5
625 μ s–0.25 s	200 t ^{0.5}
> 0.25 s	100

*The angular subtense (α_{\max}) of an extended source beyond which additional subtense does not contribute to the hazard.

t: exposure duration

Data sources: (1) American National Standards Institute. *Safe Use of Lasers*. Orlando, FL: Laser Institute of America; 2014. ANSI Z136.1-2014. (2) International Electrotechnical Commission. *Safety of Laser Products, Part 1: Equipment Classification and Requirements*. 3rd ed. Geneva, Switzerland: IEC; 2014. IEC 60825-1-2014. (3) Guidelines on limits of exposure to laser radiation of wavelengths between 180 nm and 1000 nm. *Health Phys*. 2013;105(3):271–295.

Bp, Schulmeister et al proposed the formulation shown in Table 10-17 and Figure 10-13 for α_{\max} as a function of exposure duration.^{65,66} Note that the minimum value of α_{\max} is set at 5 mrad, while α_{\min} continues to be equal to 1.5 mrad. Because the formulation of C_E would remain unchanged, the MPE would always scale with α in the range from 1.5 to 5 mrad (Figure 10-14).

Given this formulation, the value of α_{\max} is 5 mrad for exposures less than 625 μ s, and the MPE at α_{\max} is 3.3 times the point-source MPE. Unfortunately, this produces values for the MPE that for certain cases are essentially equal to the experimental ED₅₀ (Figure

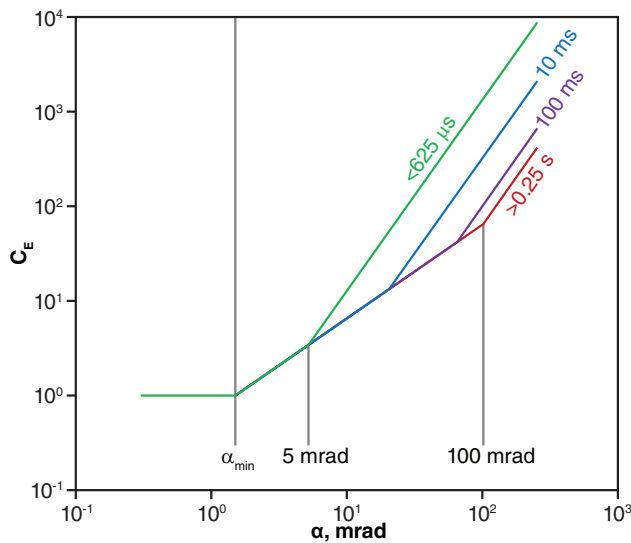


Figure 10-14. Impact on correction factor C_E (C_6 in IEC) for different pulse durations when the maximum angular subtense (α_{\max}) is time dependent.

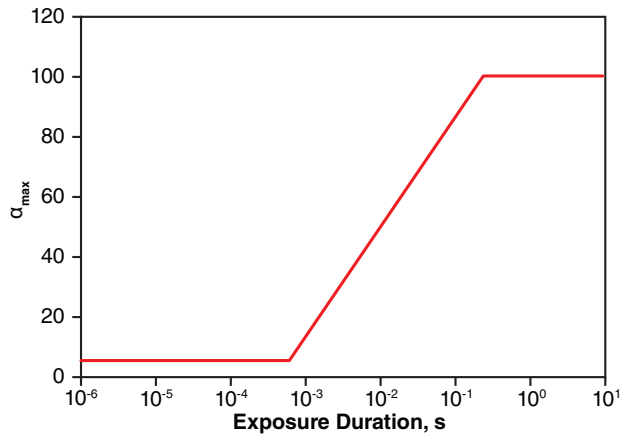


Figure 10-13. A proposed dependence of the maximum angular subtense (α_{\max}) on exposure duration. This proposal was accepted by the American National Standards Institute, International Commission on Non-Ionizing Radiation Protection, and International Electrotechnical Commission in 2013 and 2014.

10-15). This brought into question the value of the pre-2013 MPE at α_{\min} .

Figure 10-16 shows that the pre-2013 guidelines provided a margin of safety for 0.1 s exposures, even given the possibility that the point-source ED₅₀ might be

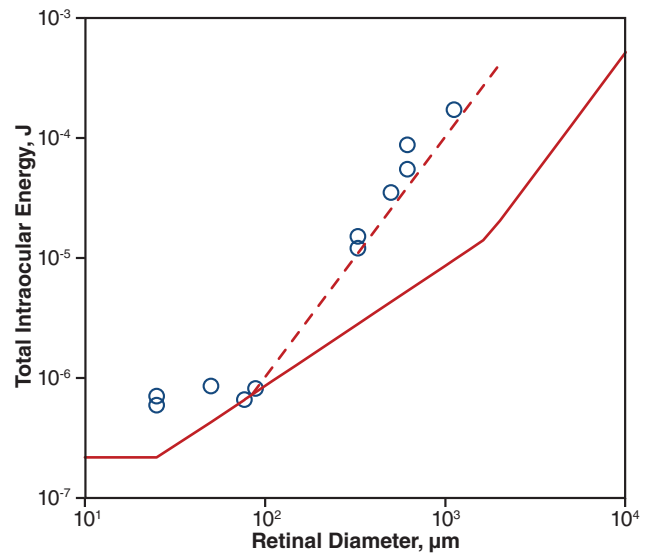


Figure 10-15. The effect of setting the maximum angular subtense (α_{\max}) at 5 mrad for exposure durations below 625 μ s. The resulting maximum permissible exposure would be almost equal to the ED₅₀ data of Zuclich et al¹ for retinal irradiance diameters greater than 85 μ m (5 mrad).

(1) Zuclich JA, Edsall PR, Lund DJ, et al. New data on the variation of laser-induced retinal damage threshold with retinal image size. *J Laser Applications*. 2008;20(2):83–88.

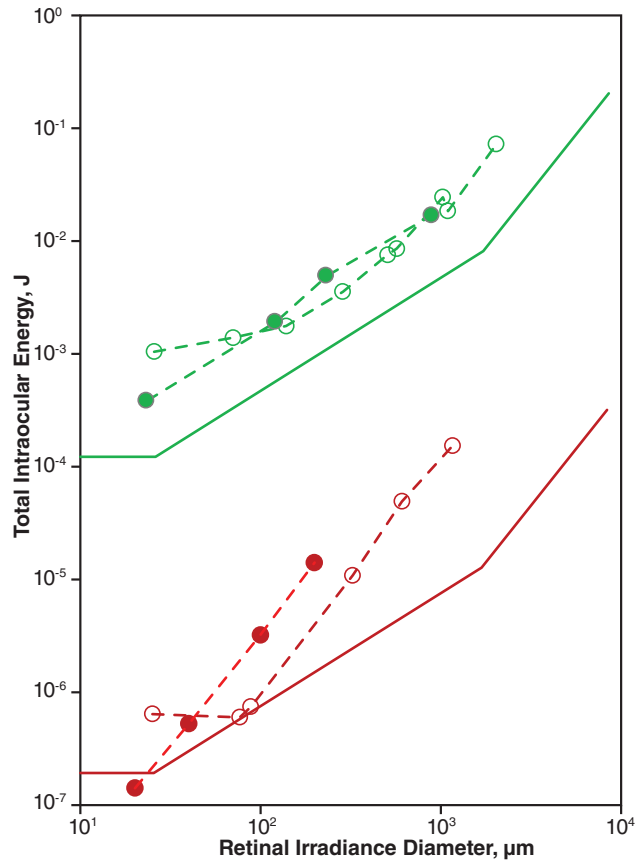


Figure 10-16. A comparison of the dependence of ED_{50} on irradiance diameter for in-vivo exposures (monkey eyes) and in-vitro exposures (retinal explants). Shown are 24-h endpoint ED_{50} data for 514 nm, 0.1 s duration macular exposures in monkeys (open green circles)¹; cell death endpoint ED_{50} data for 532 nm, 0.1 s duration exposures in retinal explants (closed green circles)²; 24-h endpoint ED_{50} data for 532 nm, 5 ns duration macular exposures in monkeys (open red circles)³; and cell death endpoint ED_{50} data for 532 nm, 100 ps duration exposures in retinal explants (closed red circles).⁴ The pre-2013 maximum permissible exposure for 0.1 s exposure duration (solid green line) and for 5 ns and 100 ps exposure duration (solid red line) are included for comparison.

(1) Lund DJ, Edsall PR, Stuck BE, Schulmeister K. Variation of laser-induced retinal injury with retinal irradiated area: 0.1 s, 514 nm exposures. *J Biomed Opt.* 2007;12(2):06180. (2) Schulmeister K, Husinski J, Seiser B, et al. Ex vivo and computer model study on retinal thermal laser induced damage in the visible wavelength range. *J Biomed Opt.* 2008;13(5):054038. (3) Zuclich JA, Edsall PR, Lund DJ, et al. New data on the variation of laser-induced retinal damage threshold with retinal image size. *J Laser Applications.* 2008;20(2):83–88. (4) Roegen J, Lin CP. Photomechanical effects—experimental studies of pigment granule absorption, cavitation and cell damage. *SPIE.* 2000;3902:35–40.

lower than that obtained through in-vivo experiments. There is no compelling reason to change the form of C_E for CW exposures. On the other hand, the pre-2013 guidelines did not provide a safety margin for 5 ns, 532 nm exposures. It is evident that the provisions of those guidelines must be adjusted for short-pulse exposures. As noted above, an indicated adjustment would change the form of C_E such that the MPE for short-pulse exposures varied with D^2 for $D > 85 \mu\text{m}$ (5 mrad) (see Figure 10-14). Such a change results in MPEs that are a better fit to the data for $D > 85 \mu\text{m}$, but it creates a problem with safety margins.²⁶ To provide a margin of safety for large D s, while at the same time maintaining the point-source MPE at the current level, would require that D_{\min} be increased to 80 to 100 μm (Figure 10-17). This formulation is supported by the in-vivo threshold data, but not by thermal models or in-vitro threshold data, and it is difficult to reconcile with the known visual acuity of primate eyes.

In-vivo bioeffects data certainly suggest that the value of α_{\min} might be set too low. The data in Figure 10-3 strongly suggest that the ED_{50} (TIE) does not decrease with α for α s less than ~ 5 mrad, and setting the value of α_{\min} to 5 mrad would be a better fit to the in-vivo data. Note that in order to make such a change in α_{\min} , it is essential both to understand why the ED_{50} reaches a minimum at that value, and to rule out as causal any experimental limitation that might not be operant for human exposure. In-vitro experiments with eye explants or cell cultures show that the threshold for damage at the RPE level does continue to decrease with irradiance diameter below 100 μm when all the uncertainties associated with imaging through the preretinal ocular media are removed (see Figure 10-16). These factors, which were discussed in the preceding sections, might operate differently in the optically immobilized eye of an anesthetized animal than in the fully active and accommodating eye of an alert young human. Lund et al addressed the role of uncompensated aberrations in the eye of the anesthetized animal during in-vivo injury threshold experiments by using an adaptive-optics-based wavefront correction system incorporated into the exposure configuration.⁶⁷ A wavefront analyzer detected the aberrations of the animal eye and drove an adaptive optics mirror to pre-distort the laser beam to compensate for those aberrations. In theory, a near-diffraction-limited spot size should result at the retina, and, if the retinal injury thresholds were purely radiant-exposure dependent, the injury threshold would be reduced by an order of magnitude compared to the threshold in the uncompensated eye. However, the experimental results produced an injury threshold reduction of only about 30%. The authors concluded

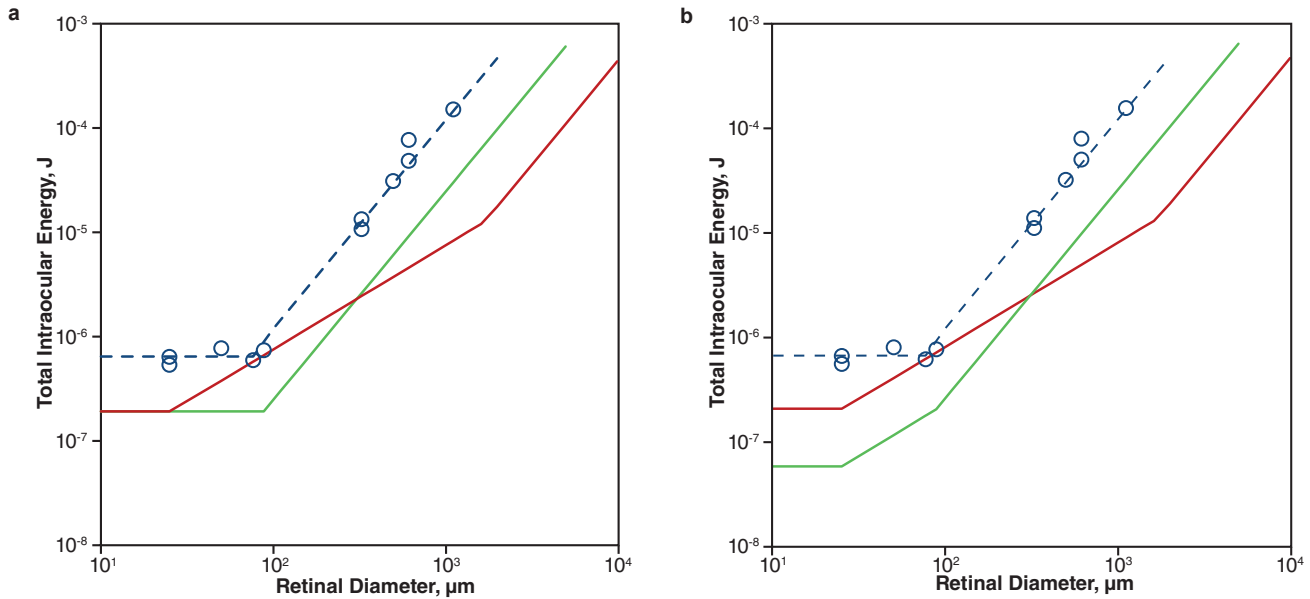


Figure 10-17. Possible changes to the ns-to-ms-duration maximum permissible exposure (MPE) to reflect the D^2 dependence of thresholds for large irradiance diameters while providing a margin of safety at all irradiance diameters: (a) an increase in D_{\min} (α_{\min}) or (b) a decrease in the point-source MPE. This was the basis for the 2014 revision of the American National Standards Institute and International Electrotechnical Commission standards. Macular ED_{50} data (blue) is for 5 ns exposures at 532 nm.¹ The pre-2013 MPE is shown in red. Proposed changes to the MPE are shown in green.

(1) Zuclich JA, Edsall PR, Lund DJ, et al. New data on the variation of laser-induced retinal damage threshold with retinal image size. *J Laser Applications*. 2008;20(2):83–88.

that the fact that the measured injury thresholds did not decrease for irradiance diameters below 100 μm was not a result of uncompensated aberrations, but rather was likely due to difficulty in detecting the very small areas of injury in vivo unless the radiant exposure was substantially increased.

If the value of D_{\min} remains at 25 μm , then the value of the point-source MPE in the nanosecond-pulse-duration regime must decrease substantially. This choice is supported by thermal models and by the in-vitro data. A reevaluation and augmentation of the in-vivo ED_{50} values for point-source exposures in the 1 ns to 1,000 ns time range also supports the need to decrease the point-source MPE by a factor of ~ 3 in this exposure duration range.⁶⁸

After considering the new data and interpretations summarized in this chapter, ICNIRP⁶⁹ chose to adopt the time-varying α_{\max} in the form proposed by Schulmeister^{65,66} and shown in Table 10-17 and Figure 10-14. At the same time, ICNIRP accepted the need to decrease the value of the 0.01 ns to 5 μm MPE at α_{\min} by a factor of 2.5 to provide a more adequate safety margin for short-pulse exposures. Together, these changes provide a much better match of the MPE to the ED_{50} data over all exposure durations.⁷⁰ The changes adopted by ICNIRP have been accepted by both ANSI and IEC and are incorporated into the latest editions of ANSI Z136.1⁷¹ and IEC 60825-1.⁷²

SUMMARY

For lasers in the retinal hazard wavebands, the relationship between the threshold for thermally induced injury of the retina and the size and shape of the retinal image is centrally important to the understanding and application of laser safety exposure limits. Early safety standards assumed that the retinal injury threshold varied with the square of the diameter of the beam on the retina; therefore, the standards said that the MPE should vary with the square of the

angle subtended by the beam on the retina. However, further laser-induced injury threshold studies led to the perception that the retinal injury threshold varied directly with the diameter of the beam on the retina; therefore, the safety standards were revised to provide guidance that the MPE should vary directly with the angle subtended by the beam on the retina. From a theoretical point of view, neither of these formulations was satisfactory.

This chapter reexamined the relevant old and new bioeffects data relating the laser-induced retinal injury thresholds to the diameter of the laser beam on the retina, and noted that injury threshold varied with the square of the diameter for short-duration exposures but varied directly with the diameter for longer-duration exposures. Thermal models of laser-induced retinal injury provided a better understanding of the dynamics of this dependence and led to

the formulation of a time-varying α_{\max} . This in turn effectively provided a transition from a diameter-squared dependence of the MPE for short-duration exposures to a diameter dependence of the MPE for longer-duration exposures. This new formulation, which has been incorporated into the latest editions of the laser safety standards, provides a consistent relationship between the MPE and laser-induced injury thresholds.

REFERENCES

1. Roegen J, Lin CP. Photomechanical effects—experimental studies of pigment granule absorption, cavitation and cell damage. *SPIE*. 2000;3902:35–40.
2. King RG, Geeraets WT. The effect of Q-switched ruby laser on retinal pigment epithelium *in vitro*. *Acta Ophthalmol*. 1968;46:617–631.
3. Mills BM, Connor TM, Foltz MS, et al. Microcavitation and spot size dependence for damage of artificially pigmented hTERT-RPE1 cells. *SPIE*. 2004;5319:217–223.
4. Schulmeister K, Husinski J, Seiser B, et al. Ex vivo and computer model study on retinal thermal laser-induced damage in the visible wavelength range. *J Biomed Opt*. 2008;13(5):054038.
5. Lund DJ, Lund BJ. The determination of laser-induced injury thresholds. In: *Proceedings of the International Laser Safety Conference*. Albuquerque, NM: Laser Institute of America; 2015: 69–73.
6. Lee H, Alt C, Pitsillides CM, Lin CP. Optical detection of intracellular cavitation during selective laser targeting of the retinal pigment epithelium: Dependence of cell death mechanism on pulse duration. *J Biomed Opt*. 2007;12(6):064034.
7. Schuele G, Rumohr M, Huettmann G, Brinkman R. RPE damage thresholds and mechanisms for laser exposure in the microsecond-to-millisecond time regimen. *Invest Ophthalmol Vis Sci*. 2005;46(2):714–719.
8. Schulmeister K, Sonneck G, Hödlmoser H, Rattay F, Mellerio J, Sliney DH. Modeling of uncertainty associated with dose-response curves as applied to probabilistic risk assessment in laser safety. *SPIE*. 2001;4246:155–172.
9. Sliney DH, Mellerio J, Gabel VP, Schulmeister K. What is the meaning of threshold in laser injury experiments? Implications for human exposure limits. *Health Phys*. 2002;82(3):335–347.
10. Vassiliadis A, Rosan RC, Zweng HC. *Research on Ocular Thresholds*. Menlo Park, CA: Stanford Research Institute; 1969. <https://apps.dtic.mil/dtic/tr/fulltext/u2/700422.pdf>. Accessed December 12, 2018.
11. Donnelly WJ 3rd, Roorda A. Optimal pupil size in the human eye for axial resolution. *J Opt Soc Am A Opt Image Sci Vis*. 2003;20(11):2010–2015.
12. Birngruber R, Dreschel E, Hillankamp F, Gabel VP. Minimum spot size on the retina formed by the optical system of the eye. *Int Ophthalmol*. 1979;1(3):175–178.
13. Stein MN, Elgin SS. *Measurement of Retinal Image for Laser Radiation in Rhesus Monkey*. Bethesda, MD: Eye Research Foundation; 1970.
14. Polhamus GL, Cohoon DK, Allen RG. The spread function in the rhesus. [Unpublished document, US Air Force School of Aerospace Medicine, Brooks Air Force Base, TX; 1985.]
15. Frisch GD, Dallas AC. Retinal irradiation diameter estimation. *Appl Opt*. 1972;11:939–944.

16. Beatrice ES, Frisch GD. Retinal laser damage thresholds as a function of the image diameter. *Arch Environ Health*. 1973;27:322–326.
17. Vassiliadis A, Zweng HC, Peppers NA, Peabody RR, Honey RC. Thresholds of laser eye hazards. *Arch Environ*. 1970;20:161–170.
18. Westheimer G, Campbell FW. Light distribution in the image formed by the living eye. *J Opt Soc Am*. 1962;52(9):1040–1045.
19. Krauskopf J. Light distribution in human retinal images. *J Opt Soc Am*. 1962;52(9):1046–1050.
20. Campbell RG, Gubisch RW. Optical quality of the human eye. *J Physiol*. 1966;186:558–578.
21. Williams DR, Brainard DH, McMahon MJ, Navarro R. Double-pass and interferometric measures of the optical quality of the eye. *J Opt Soc Am A Opt Image Sci Vis*. 1994;11(12):3123–3135.
22. Gubisch RW. Optical performance of the human eye. *J Opt Soc Am*. 1967;57(3):407–415.
23. Sliney DH, Freasier BC. Evaluation of optical radiation hazards. *Appl Opt*. 1973;12(1):1–24.
24. Milsom PK, Till SJ, Rowlands G. The effects of ocular aberrations on retinal damage thresholds in the human eye. *Health Phys*. 2006;91:20–28.
25. Zuclich JA, Edsall PR, Lund DJ, et al. Variation of laser-induced retinal damage threshold with retinal image size. *J Laser Applications*. 2000;12(2):74–80.
26. Lund DJ, Edsall PR, Stuck BE, Schulmeister K. Variation of laser-induced retinal injury with retinal irradiated area: 0.1 s, 514 nm exposures. *J Biomed Opt*. 2007;12(2):06180.
27. Zuclich JA, Edsall PR, Lund DJ, et al. New data on the variation of laser-induced retinal damage threshold with retinal image size. *J Laser Applications*. 2008;20(2):83–88.
28. American National Standards Institute. *Safe Use of Lasers*. Cincinnati, OH: Laser Institute of America; 1983. ANSI Standard Z136.1-1983.
29. Henderson R, Schulmeister K. *Laser Safety*. Philadelphia, PA: Institute of Physics Publishing; 2004.
30. American National Standards Institute. *Safe Use of Lasers*. Orlando FL: Laser Institute of America; 2007. ANSI Z136.1-2007.
31. Revision of guidelines on limits of exposure to laser radiation of wavelengths between 400 nm and 1.4 μm . *Health Phys*. 2000;29(4):431–440.
32. International Electrotechnical Commission. *Safety of Laser Products, Part 1: Equipment Classification, Requirements and Users Guide*. 2nd ed. Geneva, Switzerland: IEC; 2007. IEC 60825-1-2007.
33. Allen RG, Bruce WR, Kay KR, et al. *Research on Ocular Effects Produced by Thermal Radiation*. Brooks Air Force Base, TX: US Air Force; 1967. Final Report AF41(609)-3099, AD659146.
34. Ham WT Jr, Wisenger H, Schmidt FH, et al. Flash burns in the rabbit retina as a means of evaluating the retinal hazard from nuclear weapons. *Am J Ophthalmol*. 1958;46:700–723.
35. Jacobson JH, Cooper B, Najac HW. *Effects of Thermal Energy on Retinal Function*. Wright-Patterson Air Force Base, OH: Aerospace Medical Division; 1962. Air Force Systems Command Report AMRL-TDR-62-96.
36. Ham WT Jr, Williams RC, Mueller HA, Guerry D 3rd, Clarke AM, Geeraets WJ. Effects of laser radiation on the mammalian eye. *Trans N Y Acad Sci*. 1966;28:517–526.

37. Vassiliadis A, Rosan RC, Peabody RR, Zweng HC, Honey RC. *Investigations of Retinal Damage Using a Q-switched Ruby Laser (AD489476)*. Menlo Park, CA: Stanford Research Institute; 1966.
38. Beatrice ES, Shawaluk PD. *Q-Switched Neodymium Laser Retinal Damage in Rhesus Monkey*. Philadelphia, PA: Frankford Arsenal; 1973. Report No. M73-9-1.
39. Borland RG, Brennan DH, Marshall J, Viveash JP. The role of fluorescein angiography in the detection of laser-induced damage to the retina: A threshold study for Q-switched neodymium and ruby lasers. *Exp Eye Res.* 1978;27:471–493.
40. Goldman AI, Ham WT Jr, Mueller HA. Ocular damage thresholds and mechanisms for ultrashort pulses of both visible and infrared laser radiation in the rhesus monkey. *Exp Eye Res.* 1977;24:45–56.
41. Greiss GA, Blankenstein MF, Williford GG. Ocular damage from multiple-pulse laser exposure. *Health Phys.* 1980;39:921–927.
42. Ham WT Jr, Geeraets WT, Mueller HA, Williams RC, Clarke AM, Cleary SF. Retinal burn thresholds for the helium-neon laser in the rhesus monkey. *Arch Ophthalmol.* 1970;84:797–809.
43. Lund DJ, Beatrice ES. Ocular hazards of short-pulse argon laser irradiation. *Health Phys.* 1979;36:7–11.
44. Zuclich JA, Blankenstein MF. *Additivity of Retinal Damage for Multiple Pulse Laser Exposures*. San Antonio, TX: KRUG International; 1988. US Air Force School of Aerospace Medicine Report No. TR-88-24.
45. Lund DJ. *Variation of ED_{50} With Retinal Irradiance Diameter - 850 nm Erbium Laser*. San Francisco, CA: Letterman Army Institute of Research; 1977. Laboratory Notebook U0023-G.
46. Lund DJ. *Variation of ED_{50} With Retinal Irradiance Diameter - 599 nm Flashlamp-Pumped Dye Laser*. San Francisco, CA: Letterman Army Institute of Research; 1979. Laboratory Notebook U0023-G.
47. Zuclich JA, Lund DJ, Edsall PR, et al. Experimental study of the variation of laser-induced retinal damage with retinal image size (microsecond pulsewidths). *Nonlinear Opt.* 1999;21:18–27.
48. Cain CP, Toth CA, Noojin GD, et al. Visible lesion threshold dependence on retinal spot size for femtosecond laser pulses in the primate eye. *J Laser Applications.* 2001;13(3):125–131.
49. Takata AN, Goldfinch L, Hinds JK, Kuan LP, Thomopoulos N, Weigandt A. *Thermal Model of Laser-Induced Eye Damage*. Chicago, IL: IIT Research Institute; 1974.
50. Hansen W, Fine S. Melanin granule models for pulsed laser induced retinal injury. *Appl Optics.* 1968;71:155–159.
51. Hayes JR, Wolbarsht M. Thermal model for retinal damage induced by pulsed lasers. *Aerosp Med.* 1968;39:474–480.
52. Hayes JR, Wolbarsht M. Models in pathology: Mechanisms of action of laser energy with biological tissues. In: Wolbarsht M, ed. *Laser Applications in Medicine and Biology*. New York, NY: Plenum Press; 1971: 255–274.
53. Zeltov G, Glaskov V, Podol'tzef A, Linnik L, Privalov A. Retinal damage from intense visible light. *Health Phys.* 1989;56:625–630.
54. Thompson CR, Gerstman BS, Jacques SL, Rogers ME. Melanin granule model for laser-induced thermal damage in the retina. *Bull Math Biol.* 1996;58(3):513–553.
55. Schulmeister K, Seiser B, Edthofer F, Lund DJ. Modelling of the laser spot size dependence of retinal thermal damage. In: *Proceedings of the International Laser Safety Conference (ILSC)*. Orlando, FL: Laser Institute of America; 2005: 48–57.
56. Pearce J, Thomsen S. Rate process analysis of thermal damage. In: Welch AJ, Van Gemert MJC, eds. *Optical-Thermal Response of Laser-Irradiated Tissue*. New York, NY: Plenum Press; 1995: 561–606.

57. Kennedy PK, Zuclich JA, Lund DJ, et al. Laser-induced retinal damage thresholds for annular retinal beam profiles. *SPIE*. 2004;5319:258–266.
58. Till SJ, Milsom PK, Rowlands G. A new model for laser-induced thermal damage in the retina. *Bull Math Biol*. 2003;65:731–746.
59. Kennedy PK, Druessell JJ, Cupello JM, et al. Parameter sensitivity of the thompson granular retinal damage model. *SPIE*. 1998;3524:146–154.
60. Jean M, Schulmeister K. Validation of a computer model to predict laser induced thermal injury thresholds of the retina. In: *Proceedings of the International Laser Safety Conference (ILSC)*. Orlando, FL: Laser Institute of America; 2013: 229–238.
61. Lin CP, Kelly MW, Sibayan SAB, Latina MA, Anderson RR. Selective cell killings by microparticle absorption of pulsed laser radiation. *IEEE J Select Topics Quantum Electron*. 1999;5(4):963–968.
62. Brinkmann R, Hüttmann G, Roegerer J, Roeder J, Birngruber R, Lin CP. Origin of retinal pigment epithelial cell damage by pulsed laser irradiance in the nanosecond to microsecond time regimen. *Lasers Surg Med*. 2000;27:451–464.
63. Hollins RC. Optical limiters—spatial and temporal effects. *Nonlinear Opt*. 1999;21:49–61.
64. Riehl D, Deshays T, Andrieux M, Lafonta F. Evaluation of the efficiency of optical limiters by a convolution method. Paper presented at: Laser Bioeffects Meeting; June 13, 2002; Paris, France.
65. Schulmeister K, Stuck BE, Lund DJ, Sliney DH. Review of thresholds and exposure limits for laser and broadband optical radiation for thermally induced retinal injury. *Health Phys*. 2011;100(2):210–220.
66. Schulmeister K, Stuck BE, Lund DJ, Sliney DH. Proposed changes for the retinal thermal MPE. In: *Proceedings of the International Laser Safety Conference (ILSC)*. Orlando, FL: Laser Institute of America; 2007: 121–127.
67. Lund BJ, Lund DJ, Edsall PR. Laser-induced retinal damage threshold measurements with wavefront correction. *J Biomed Opt*. 2008;13(6):064011.
68. Lund BJ, Lund DJ, Holmes ML. Retinal damage thresholds in the 1 ns to 100 ns exposure duration range. In: *Proceedings International Laser Safety Conference (ILSC)*. San Jose, CA: Laser Institute of America; 2011: 183–186.
69. Guidelines on limits of exposure to laser radiation of wavelengths between 180 nm and 1000 nm. *Health Phys*. 2013;105(3):271–295.
70. Lund DJ. The new maximum permissible exposure: A biophysical basis. In: Barret K, ed. *Laser Safety: Tools and Training*. 2nd ed. Boca Raton, FL: CRC Press; 2014: 145–175.
71. American National Standards Institute. *Safe Use of Lasers*. Orlando, FL: Laser Institute of America; 2014. ANSI Z136.1-2014.
72. International Electrotechnical Commission. *Safety of Laser Products, Part 1: Equipment Classification and Requirements*. 3rd ed. Geneva, Switzerland: IEC; 2014. IEC 60825-1-2014.